



**HAL**  
open science

## Sense of agency for intracortical brain–machine interfaces

Andrea Serino, Marcia Bockbrader, Tommaso Bertoni, Sam Colachis Iv, Marco Solcà, Collin Dunlap, Kaitie Eipel, Patrick Ganzer, Nick Annetta, Gaurav Sharma, et al.

► **To cite this version:**

Andrea Serino, Marcia Bockbrader, Tommaso Bertoni, Sam Colachis Iv, Marco Solcà, et al.. Sense of agency for intracortical brain–machine interfaces. *Nature Human Behaviour*, 2022, 10.1038/s41562-021-01233-2. hal-03537274

**HAL Id: hal-03537274**

**<https://hal.science/hal-03537274>**

Submitted on 20 Jan 2022

**HAL** is a multi-disciplinary open access archive for the deposit and dissemination of scientific research documents, whether they are published or not. The documents may come from teaching and research institutions in France or abroad, or from public or private research centers.

L'archive ouverte pluridisciplinaire **HAL**, est destinée au dépôt et à la diffusion de documents scientifiques de niveau recherche, publiés ou non, émanant des établissements d'enseignement et de recherche français ou étrangers, des laboratoires publics ou privés.

## Sense of Agency for intracortical brain machine interfaces

Andrea Serino<sup>\*1,2</sup>, Marcie Bockbrader<sup>\*3</sup>, Tommaso Berton<sup>1</sup>, Sam Colachis<sup>3p,4c</sup>, Marco Solca<sup>2</sup>, Collin Dunlap<sup>3,4</sup>, Kaitie Eipel<sup>3p</sup>, Patrick Ganzer<sup>4</sup>, Nick Annetta<sup>4</sup>, Gaurav Sharma<sup>4p,9c</sup>, Pavo Orepic<sup>2</sup>, David Friedenberg<sup>4</sup>, Per Sederberg<sup>5</sup>, Nathan Faivre<sup>2,6</sup>, Ali Reza<sup>\*\*7</sup>, Olaf Blanke<sup>\*\*2,8</sup>

<sup>1</sup>MySpace Lab, Department of Clinical Neuroscience, University Hospital Lausanne (CHUV), Lausanne, Switzerland; <sup>2</sup>Laboratory of Cognitive Neuroscience, Brain Mind Institute & Center for Neuroprosthetics, Ecole Polytechnique Fédérale de Lausanne (EPFL), Campus Biotech, Geneva, Switzerland; <sup>3</sup>Department of Physical Medicine and Rehabilitation, The Ohio State University, Columbus, Ohio, US; <sup>4</sup>Medical Devices and Neuromodulation, Battelle Memorial Institute, Columbus, Ohio, US; <sup>5</sup>Department of Psychology, University of Virginia, Charlottesville, Virginia, US; <sup>6</sup>Univ. Grenoble Alpes, Univ. Savoie Mont Blanc, CNRS, LPNC, 38000 Grenoble, France; <sup>7</sup>Rockefeller Neuroscience Institute, West Virginia University, Morgantown, West Virginia, US; <sup>8</sup>Department of Neurology, University Hospital, Geneva, Switzerland; <sup>9</sup>Air Force Research Laboratory, Dayton, Ohio, US.

\* These authors contributed equally; \*\* These authors jointly supervised this work.  
<sup>p</sup> prior affiliation at time of work; <sup>c</sup> current affiliation

\* These authors contributed equally; \*\* These authors jointly supervised this work.

Corresponding authors:

Andrea Serino - [andrea.serino@unil.ch](mailto:andrea.serino@unil.ch)

Olaf Blanke – [olaf.blanke@epfl.ch](mailto:olaf.blanke@epfl.ch)

43 **Abstract**

44 Intracortical brain machine interfaces decode motor commands from neural signals and  
45 translate them into actions, enabling movement for paralyzed individuals. The subjective  
46 sense of agency associated to actions generated via intracortical brain machine  
47 interfaces, the involved neural mechanisms and its clinical relevance are currently  
48 unknown. By experimentally manipulating the coherence between decoded motor  
49 commands and sensory feedback in a tetraplegic individual using a brain machine  
50 interface, we provide evidence that primary motor cortex processes sensory feedback,  
51 sensorimotor conflicts and subjective states of actions generated via the brain machine  
52 interface. Neural signals processing the sense of agency affected the proficiency of the  
53 brain machine interface, underlining the clinical potential of the present approach.  
54 These findings show that primary motor cortex encodes information related to action  
55 and sensing, but also sensorimotor and subjective agency signals, which in turn are  
56 relevant for clinical applications of brain machine interfaces.

57  
58  
59  
60  
61  
62  
63  
64  
65  
66  
67  
68  
69  
70  
71  
72  
73  
74

75 **Main text**

76

77 **Introduction**

78 When performing a voluntary movement, motor commands from the brain activate body  
79 effectors, which produce a cascade of reafferent sensory (proprioceptive, tactile, visual)  
80 cues. Motor commands are also associated with prediction signals about the sensory  
81 consequences of the movement. The congruency between motor commands, reafferent  
82 sensory feedback, and sensory predictions is at the basis of the sense of agency, our  
83 feeling of being in control of our actions<sup>1-3</sup>. In case of damage to the motor system,  
84 motor commands that would trigger actions do not reach body effectors, leading to  
85 different types of paralysis, depending on the location and severity of damage.  
86 Intracortical brain machine interfaces (BMI) bypass such brain-body disconnection by  
87 decoding brain signals from different regions (i.e., primary motor cortex (M1), parietal or  
88 premotor cortex) and translating them into motor commands for the control of robots,  
89 exoskeletons<sup>4,5</sup>, neuromuscular functional electrical stimulation<sup>6,7</sup> or other devices<sup>8</sup>,  
90 enabling different actions (BMI actions) for patients with severe neuromotor  
91 impairments<sup>9</sup>.

92

93 Here we study how it feels to generate movements with an intracortical-BMI, that is  
94 what is the sense of agency for BMI actions ((see <sup>10,11</sup> for recent studies with non-  
95 invasive brain computer interfaces (BCI)) and search for a potential neural mechanism.  
96 In particular, we asked whether motor neurons in human M1 encode not only motor  
97 commands, but also sensory feedback and whether these signals covary with agency  
98 for BMI actions Finally we tested whether agency also affects the efficiency of the BMI  
99 system - i.e. whether agency has a potential therapeutic benefit.

100

101 We applied classic approaches from psychophysics, neurophysiology,  
102 neuroengineering and virtual reality (VR) to ask these questions in a patient suffering  
103 from tetraplegia (caused by severe cervical spinal cord injury; C5/C6), who had been a  
104 BMI expert for two years before the start of the present study<sup>6</sup>. The patient had no  
105 preserved motor function below the C5 level. His sensory functions were extremely

106 limited and only showed partially preserved function at the C6 level on the left side and  
107 at C5 on the right side (there was also residual sensation for pressure on his right  
108 thumb). Concerning proprioception, he had preserved perception for shoulder, elbow  
109 and wrist joint position, but no proprioception for digits joint position (see Material and  
110 methods for more details).

111  
112 The BMI consisted of a 96-channel array implanted in the hand area of left M1 and  
113 actuated a transcutaneous forearm neuromuscular electrical stimulation (NMES) system  
114 (see <sup>6</sup> for a full description of the system) to translate decoded cortical signals into right  
115 forearm and hand movements. In order to study the sense of agency for BMI actions  
116 and to evaluate its clinical impact, we experimentally manipulated the congruency  
117 between the decoded actions and the actions actuated by the BMI-NMES system. As  
118 illustrated in Figure 1, the participant was instructed to realize a cued action with the  
119 BMI and was provided with movement-related sensory feedback using visual (via VR)  
120 and/or somatosensory (via NMES) stimulation. Critically, this feedback was either  
121 congruent or incongruent with respect to the motor commands decoded from M1: half of  
122 the trials, in which the decoded action corresponded to the cued action (e.g., open  
123 hand), were associated with congruent feedback (e.g., open hand), while the other half  
124 were associated with incongruent feedback (e.g. the opposite action: close hand). For  
125 each BMI action, we asked the participant whether he felt in control of that action and to  
126 rate his confidence about this judgement, allowing us to (1) gauge the sense of agency  
127 for BMI actions and how this was modulated by the congruency between motor  
128 commands and sensory feedback. Next, neural data from the M1 implant were analyzed  
129 to measure how (2) the sense of agency and (3) sensory feedback were encoded in the  
130 activity of M1 neurons, quantified as multi-unit (MU) firing rates and local field potentials  
131 (LFP). Finally, we investigated (4) how visual and somatosensory feedback, and the  
132 associated sense of agency, affected the performance of the BMI system by changing  
133 the pattern of response of M1 neurons. By investigating what it feels like to control  
134 actions mediated by an intracortical BMI, our data show neural patterns in M1 activity  
135 (MU and LFP) reflecting the processing of agency for BMI actions, as generated by the  
136 congruency between intention and sensory feedback. Importantly, we show that the  
137 nature of somatosensory feedback (and the related sense of agency) affected the

138 efficiency of the BMI system by modulating the response properties of M1 neurons,  
139 underlining the clinical relevance of sensory feedback and agency for the BMI field.

140

141 During the experiment, the participant was cued to execute one of four target actions  
142 (hand opening, hand closing, thumb extension, thumb flexion) using a validated BMI  
143 neuroprosthesis. Neural activity corresponding to each target movement was recorded  
144 via a 96-channel microelectrode array in M1 and a nonlinear support vector machine  
145 classifier was applied to decode the participant's chosen action from MU activity (see <sup>6</sup>  
146 for full description). On each trial, the classifier provided the likelihood of each target  
147 action (on a -1 to +1 range, in 100 ms bins), thus decoding one of the four target actions  
148 from the participant's M1 activity. In three different experiments, visual, somatosensory,  
149 or visual-somatosensory feedback about the BMI action was provided (Figure 1). In  
150 Experiment 1, VR was used to provide visual feedback, consisting of a life-size virtual  
151 arm on a monitor superimposed over the participant's right arm, matching the location  
152 and dimensions of the participant's real arm, which was occluded from view. In  
153 Experiment 2, NMES was used to provide 'somatosensory' feedback: the patient's  
154 upper limb muscles were electrically stimulated so he could feel, but not see the  
155 selected movement. Experiment 3 combined VR and NMES to provide 'visual-  
156 somatosensory feedback' (see below). In half of the trials, sensory feedback was  
157 congruent with the cued action, while in the other half it was incongruent (i.e., the  
158 opposite, action was executed) (see Figure 1B). At the end of each trial, we gauged the  
159 participant's sense of agency (0 or 1; Q1) and confidence (rating between 0 and 100;  
160 Q2). Importantly, the amount of sensory information was kept constant across  
161 experiments, by providing non-informative sensorimotor feedback in Experiment 1 (i.e.,  
162 a pattern of NMES triggering no BMI action) and non-informative visual feedback in  
163 Experiment 2 (i.e., a static visual hand performing no action).

164

165

## 166 **Results**

167 **Sensory feedback determines agency and confidence.** Agency ratings were  
168 collected in a total of 844 trials (155, 243 and 448 trials for Experiments 1, 2 and 3,  
169 respectively; for Experiment 3 see below and Supplementary Information) and

170 compared across feedback conditions using permutation tests. A null distribution of the  
171 mean agency rating was created by shuffling the condition labels over 10'000 iterations.  
172 P-values (2-sided) were estimated by counting the proportion of shuffled samples  
173 exceeding the observed average difference across conditions. As expected, and as  
174 shown in Figure 2A, we were able to manipulate agency and confidence for BMI  
175 actions. Thus, congruent visual (Experiment 1, 93.8% (bootstrapped 95% confidence  
176 interval 93.4% - 94.2%) and 5.2% (4.8% - 5.6%) of positive responses to Q1 for  
177 congruent and incongruent trials, respectively,  $p < .0001$ ) and congruent somatosensory  
178 (Experiment 2, 97.5% (97.3% - 97.6%) and 8.8% (8.4% - 9.1%) of positive responses  
179 for congruent and incongruent trials respectively,  $p < .0001$ ) feedback resulted in more  
180 frequent agency responses versus incongruent conditions. Analyzing the role of  
181 feedback for confidence ratings (irrespective of the agency ratings), we found that  
182 confidence was modulated by somatosensory congruency (Experiment 2, Q2 ratings  
183 were higher for somatosensory congruent [M = 74.0 (73.9 - 74.2)] than incongruent [M =  
184 65.0 (64.8 - 65.2)] feedback;  $p < 0.001$ ). The effect of visual congruency on confidence  
185 ratings was not significant (Experiment 1, mean Q2 rating = 70.9 (70.6 - 71.1) for  
186 congruent, 73.4 (73.1 - 73.6) for incongruent trials;  $p = 0.28$ ).

187  
188 In order to disentangle the role of visual and somatosensory cues for agency and  
189 confidence, Experiment 3 combined VR and NMES including combinations of congruent  
190 and incongruent visual and somatosensory feedback (Figure 1). Most relevant are the  
191 comparisons between feedback conditions in which visual (V) and somatosensory (S)  
192 signals were both congruent (+) or both incongruent (-) (V+/S+; V-/S-) or when feedback  
193 was congruent in one modality and incongruent in the other modality (V+/S-; V- /S+).  
194 Results revealed that somatosensory congruency was more effective in driving the  
195 sense of agency and the associated confidence: ratings were higher not only when both  
196 feedback signals were congruent (Q1 = 100% "Yes", mean Q2 = 83.98 [83.7 - 84.0]) as  
197 compared to both being incongruent (Q1 = 7.6% "Yes" [7.2% - 7.9%], mean Q2 = 72.4  
198 [72.2 - 72.6]), both  $p$ -values  $< 0.001$ ), but also in the V- /S+ (Q1 = 68.9% "Yes" [68.4% -  
199 69.4%], mean Q2 = 59.4 [59.3 - 59.6] as compared to the V+/S- condition (Q1 = 52.2%  
200 "Yes" [51.5% - 52.8%], mean Q2 = 54.6 [54.4 - 54.8];  $p = 0.0035$  and  $p = 0.036$ , for  
201 agency and confidence respectively) (Figure 2). Collectively, these data from

202 Experiments 1-3 show that the congruency between decoded actions and sensory  
203 feedback, especially for the somatosensory modality, alters the sense of agency and  
204 confidence for actions mediated by an intracortical BMI.

205

206 The sense of agency has been traditionally studied by presenting participants with  
207 different visuo-motor couplings<sup>2,12-15</sup>. In comparison, the role of somatosensory signals  
208 remains poorly understood<sup>16</sup>, notably because it is normally impossible to decouple  
209 motor commands, somatosensory feedback and visual feedback, with extremely rare  
210 exceptions as in deafferented patients. Here we were able to contrast feedback cues  
211 that were congruent in one modality (e.g., visual) and incongruent in the other modality  
212 (e.g., somatosensory; and vice versa) with respect to the motor command and  
213 demonstrate that somatosensory cues dominate the sense of agency and the  
214 associated confidence for BMI-NMES actions. Of note, this effect cannot be due to the  
215 presence of somatosensory cues alone, as BMI actions in the visual condition were  
216 always associated with non-informative NMES stimulation producing somatosensory  
217 sensations without generating any actions (i.e., pseudo random somatosensory  
218 feedback, see Supplementary Information). Collectively these psychophysical data in a  
219 BMI expert reveal that agency for BMI actions depends on visual and somatosensory  
220 feedback (tactile and proprioceptive input) with somatosensory cues being more  
221 relevant.

222

223 **Cortical signatures of sensory feedback in M1.** We next investigated how such  
224 sensory feedback, that modulated the sense of agency, was encoded in M1 activity. We  
225 first analyzed the LFP amplitude in the different feedback conditions across the three  
226 experiments, using a regularized generalized linear model (ridge regression) and input  
227 signals from each individual channel at every time point (see Supplementary  
228 Information). As shown in Figure 3A (left), the analysis distinguished congruent vs.  
229 incongruent visual feedback (maximum Cohen's Kappa  $K = 0.40$ ,  $t\text{-sum} = 219.4$ ,  $p <$   
230  $0.001$ ) within a single period of a positive potential that lasted from ~700-1200 ms after  
231 the BMI action classification onset (Experiment 1). We could also distinguish congruent  
232 vs. incongruent somatosensory feedback (maximum Cohen's Kappa  $K = 0.64$ ,  $t\text{-sum} =$   
233  $979.8$ ,  $p < 0.001$ ) during two time periods: an early period characterized by a negative



234 potential (stronger for incongruent feedback), starting at ~200 ms after BMI  
235 classification onset, followed by a later persistent differentiation lasting almost until the  
236 end of the trial. These results were further corroborated by data from Experiment 3:  
237 congruent trials in both modalities were clearly distinguished from incongruent trials in  
238 both modalities, lasting from ~250-1900 ms after BMI classification onset (maximum  $K =$   
239  $0.66$ ,  $t\text{-sum} = 958.8$ ,  $p < 0.001$ ). In addition,  $V+/S-$  trials were different from  $V-/S+$  trials  
240 from ~300-1400 ms from BMI classification onset (maximum  $K = 0.31$ ,  $t\text{-sum} = 256.7$ ,  $p$   
241  $< 0.001$ ) (Figure 3B left). These findings show that visual and somatosensory feedback  
242 were both encoded by LFPs in human M1 and that such M1-LFP coding started earlier  
243 and was more stable over time for somatosensory feedback.

244

245 Applying the same decoding algorithm as for LFPs, we next determined if sensory  
246 feedback was also encoded by the spiking rate of MU in M1 (for methods see  
247 Supplementary Information). As shown in Figure 3A (right), in Experiment 1, MU activity  
248 distinguished between congruent and incongruent visual feedback from ~400-900 ms  
249 from BMI classification onset (max  $K$  value =  $0.41$ ,  $t\text{-sum} = 56.2$ ,  $p < .001$ ). Extending  
250 LFP findings, an earlier and more stable differentiation between congruent and  
251 incongruent somatosensory feedback was found in MU activity in Experiment 2, with an  
252 effect as early as ~200 ms from the BMI classification onset (max  $K$  value =  $0.66$ ,  $t\text{-sum}$   
253  $= 390.7$ ,  $p = < .001$ ) and then persisted from 800 to 2000 ms. Similar results were found  
254 in Experiment 3 (Figure 3B, right), where MU activity distinguished between trials  
255 congruent and incongruent in both modalities (max  $K$  value =  $0.68$ ,  $t\text{-sum} = 271.8$ ,  $p = <$   
256  $.001$ ) and between  $V+/S-$  and  $V-/S+$  trials from ~160 ms from BMI classification onset  
257 (max  $K$  value =  $0.55$ ,  $t\text{-sum} = 151.2$ ,  $p = < .001$ ). These data show that LFP and MU  
258 activity reflects visual and somatosensory feedback during actions driven by a BMI  
259 neuroprosthesis, with M1 activity early reflecting somatosensory feedback starting ~200  
260 ms after NMES activation (~150 ms after BMI classification onset, ~200 ms before M1  
261 activity encoding visual feedback) and persisting for a longer period.

262

263 The role of somatosensory and visual information is an important topic in motor control,  
264 with robust evidence showing how perturbations of sensory feedback impact motor

265 execution and adaptation<sup>17</sup>. The present data show that the congruency between an  
266 intended action and somatosensory/visual feedback is encoded by M1 neurons at  
267 different latencies. Previous studies in non-human primates described responses in M1  
268 related to tactile and visual input<sup>18,19</sup>, during active and passive movements<sup>20</sup> and during  
269 visual feedback of a pre-recorded movement<sup>21,22</sup>. The present results are consistent  
270 with proposals that suggest that M1 activity codes both for movement types and their  
271 sensory consequences, in line with recent works describing how M1 neurons encode  
272 different movement parameters (see <sup>19,23,24</sup> for reviews). Here we report that, at the  
273 population level, human M1 activity in addition discriminates between arm movements  
274 that were congruent or incongruent with the motor command, as defined by  
275 somatosensory and visual feedback, with higher accuracy, earlier and more consistent  
276 processing for the former type of sensory information. Thus, neural coding in M1  
277 contains, at the population level, information not only about the movement itself, but  
278 also about sensory consequences of actions, involving somatosensory-motor and visuo-  
279 motor loops. These results are important to explain how sensory feedback affects the  
280 proficiency of the BMI system as described below.

281

282 **Cortical signatures of the sense of agency in M1.** It is known that sensory-motor  
283 congruency is a key mechanism of agency for able-bodied actions<sup>2,3</sup>; here we have  
284 shown that this also applies to agency and confidence for BMI-mediated actions and  
285 that LFPs and MU activity in human M1 distinguishes congruent vs. incongruent BMI  
286 actions. Next, we investigated to what extent LFP and MU activity in M1 also  
287 discriminate actions with and without an accompanying sense of agency. For each trial,  
288 we sorted LFP responses as a function of whether the participant reported agency or  
289 not. As seen in Figure 4A (left), LFP activity starting ~270 ms after BMI classification  
290 onset was found to code for agency and reached a maximum information value (Max K  
291 = 0.41, t-sum = 1258.3, p < 0.001) at ~1000 ms after BMI movement onset. Thus, BMI  
292 actions for which the participant felt to be the agent were characterized by a different  
293 LFP pattern compared to BMI actions for which he did not. This was corroborated by  
294 MU activity analysis (Figure 4A, right). The MU firing rate was higher for trials with  
295 versus no agency; this discrimination started at ~300ms after BMI classification onset,

296 until 500 ms, and peaked at ~400 ms (max K = 0.45, t-sum = 232.5, p < 0.001). Later  
297 on, MU activity also differentiated for agency, with higher firing rate for trials with no  
298 agency (800-1600 ms after BMI classification). The same decoding was also able to  
299 discriminate trials with high vs. low confidence, based on a median split of Q2, from  
300 LFPs (max K = 0.296 at ~1200 ms, t-sum = 8449.3, p < 0.001) and MU (max K = 0.225  
301 at ~400 ms, t-sum = 214.9, p < 0.001).

302

303 In the experimental design, sensory feedback congruency was used to modulate the  
304 sense of agency and this may have influenced these agency findings. Accordingly, we  
305 next tested whether LFP and MU contained information related to the sense of agency  
306 per se, after controlling for the effect of sensory feedback. For this we built a continuous  
307 measure of sense of agency and confidence allowing us to regress out the effect of  
308 sensory feedback. This new index was computed by recoding confidence ratings (Q2)  
309 as -Q2, for trials with no agency (as indicated in Q1) and +Q2 for trials with agency  
310 (from Q1). This index was then orthogonalized with respect to congruency in order to  
311 regress out this effect from the agency scores. As M1 signals also varied as a function  
312 of the different cued actions (see SI), the index was also orthogonalized for the type of  
313 action. We then used the same decoder to predict orthogonalized agency scores from  
314 LFP and MU activity over time. This analysis shows that LFPs predicted the sense of  
315 agency starting at ~450 ms after BMI classification onset (max  $R^2$  = 0.03, t-sum = 69.8,  
316 p = 0.017) (see Figure 4B left). A similar pattern was found when considering MU  
317 activity, although the peak failed to reach significance after cluster-based correction for  
318 multiple comparisons (Figure 4B right). These data show that M1 activity encodes the  
319 sense of agency and associated confidence level and was modulated by the  
320 congruency between motor commands and sensory feedback. Thus, subjective mental  
321 states associated with BMI actions and control are encoded by M1 activity at the LFP  
322 level (and to a minor extent at MU), independent of the neural processing associated  
323 with sensory feedback (see Supplementary Information for single channel analyses).

324

325 **Somatosensory feedback modulates BMI classifier accuracy.** Given the strong role  
326 of sensory congruency in determining agency and its coding in M1, we finally asked

327 whether sensory feedback has any impact on the BMI classifier. To this aim, we tested  
328 whether the congruency between the decoded motor commands and sensory feedback  
329 (visual, somatosensory) affected the accuracy of the BMI classifier, defined as the  
330 summed suprathreshold activation values across a 4s window. In Experiments 1 and 2  
331 we found that congruent somatosensory feedback improved classifier accuracy ( $t(241)$   
332  $= 9.29$ , Cohen's  $d = 1.238$ ,  $p < 0.001$ ) (Figure 5B right). There was no effect due to  
333 visual feedback ( $t(153) = 1.523$ , Cohen's  $d = -0.245$ ,  $p = 0.14$ ) (Figure 5A). Moreover,  
334 incongruent somatosensory feedback was associated with lower classifier accuracy for  
335 the cued movement (Figure 5B left), and even increased classifier accuracy for the  
336 opposite movement (Figure 5B left). Thus, only somatosensory feedback congruency  
337 affected BMI accuracy in the present participant. This was extended by the results of  
338 Experiment 3, where we found a significant main effect of sensory feedback condition  
339 ( $F(3,444) = 15.83$ ,  $\eta^2 = 0.097$ ,  $p < 0.001$ ; Figure 5C). Further post-hoc corrected tests  
340 showed that the BMI classifier's accuracy was higher when feedback was congruent,  
341 than incongruent, in either modality (Tukey corrected  $t = 4.966$ , Cohen's  $d = 0.666$ ,  $p <$   
342  $0.001$ ). More interestingly, when feedback was congruent for the somatosensory  
343 modality and incongruent for the visual modality (V-/S+) BMI accuracy was higher than  
344 in the opposite feedback condition (S-/V+) ( $t = 4.558$ , Cohen's  $d = 0.612$ ,  $p < 0.001$ ).  
345 Figure 5 also shows the modulation of the BMI decoder as function of sensory feedback  
346 over time during the trial. Significant change of the decoder's output is visible from 430  
347 ms from somatosensory feedback.

348 These data from Experiments 1-3 show that BMI performance is affected by the  
349 congruency between the decoded motor commands and the somatosensory feedback  
350 induced by the action actuated by NMES. This finding is also coherent with the more  
351 reliable (i.e., earlier, more long-lasting and better decoded) processing of  
352 somatosensory feedback from M1 activity (LFP, MU). The fact that the same action as  
353 actuated by NMES (e.g., open hand) increased or decreased the BMI classifier  
354 performance, depending on whether somatosensory feedback was congruent (open  
355 hand) or incongruent (close hand) with the cued action, excludes that this effect was a  
356 generic artifact of NMES stimulation affecting the input to the BMI classifier  
357 independently from sensory information.

358 In order to better understand how somatosensory feedback affected the accuracy of the  
359 BMI classifier, we analyzed time point by time point changes in multiunit activity for the  
360 whole array. We computed the average Euclidean distance between firing patterns of  
361 trials with a given cued movement and either congruent or incongruent somatosensory  
362 feedback. For a given cued movement (e.g., movement hand open) at congruent  
363 feedback (hand open), we computed its distance either with the same movement (cued:  
364 hand open) at incongruent feedback (hand close) or with the opposite movement (hand  
365 close), at its relative incongruent feedback (hand open). This way, we compared cases  
366 with the same motor intention, but opposite sensory feedback, and trials with the  
367 opposite motor intention, but the same sensory feedback. As shown in Figure 6, trials  
368 from Experiment 2 with opposite somatosensory feedback, but the same motor  
369 intention, diverge after sensory feedback, whereas trials with opposite motor intention,  
370 but the same sensory feedback, seem to even converge slightly with respect to  
371 baseline. This shows that M1 activity after feedback reflects the movement implemented  
372 via NMES more than the intended movement, thus explaining the modulation of  
373 somatosensory feedback in BMI proficiency (see Figure 6B). As a control, we also  
374 analyzed trials with opposite motor intention and congruent somatosensory feedback.  
375 We found the activity patterns to differ only slightly with respect to trials with same  
376 somatosensory feedback, but opposite motor intention, further showing that  
377 somatosensory feedback is prevailing over motor intention after movement onset. In the  
378 case of visual feedback (Experiment 1), instead, there was no divergence of activity  
379 patterns after the feedback, while trials with different motor intention clearly diverged  
380 before the movement onset (see Figure 6A).

381  
382 In order to better display the effect of somatosensory feedback on M1 activity for each  
383 type of movements, we computed a 2D multidimensional scaling of neural activity as a  
384 function of intended movement and congruency of somatosensory feedback. This  
385 technique aims at representing the high dimensional spatio-temporal pattern of neural  
386 activity in 2D plane, while maximising the fraction of retained variance. As shown in  
387 Figure 6C, both for hand (opening/closing) and thumb (flexion/extension) movements,  
388 before sensory feedback (in the window between -650 and -150 ms before sensory  
389 feedback onset), M1 neural activity is clustered solely as a function of the intended

390 movement. After somatosensory feedback (between 0 and 600 ms from sensory  
391 feedback onset, Figure 6D), trials with congruent somatosensory feedback and a given  
392 intended movement are clustered more with trials coding for the opposite movement,  
393 but receiving the same sensory feedback rather than with trials coding for the same  
394 movement.

395 No prior study in humans and only few studies in monkeys directly tested the effects of  
396 sensory feedback on BMI performance<sup>21,25</sup>. Here we show, for the first time, an effect of  
397 feedback congruency on BMI performance, and the underlying role of M1 in this  
398 process. Our findings indicate that the recorded M1 units processed motor signals for  
399 the trained BMI actions, for sensory and sensory-motor signals reflecting the type and  
400 congruency of the sensory feedback. Importantly, these processes were found to  
401 change across time, as a function of the sensory feedback provided. In particular, our  
402 results show that, after somatosensory feedback, the pattern of neural activity from M1  
403 reflected more closely the type of movement realized by the NMES (i.e., the pattern of  
404 somatosensory feedback) rather than the intended and decoded movement. This re-  
405 writing of the encoded M1 movement as a function of the NMES-implemented  
406 movement directly relates to the improvement of BMI efficiency based on congruent  
407 somatosensory feedback that we observed and was absent in visual feedback trials.

408 This effect might be mediated by mutual connections between the primary motor and  
409 the primary somatosensory cortices, which have been extensively documented in non-  
410 humans primates<sup>26</sup> and in humans<sup>27</sup>. In addition, this effect might also depend on direct  
411 somatosensory inputs reaching M1 neurons likely from the dorsal columns via the  
412 ventrolateral thalamic nucleus<sup>28</sup>. This is an important finding, considering that original  
413 BMI approaches for severely motor-impaired patients generally provide visual feedback  
414 only<sup>5,29</sup> or somatosensory feedback by directly stimulating primary somatosensory  
415 cortex<sup>30-32</sup> (see <sup>31</sup> *for a review*). Although from a single tetraplegic participant, the  
416 present data show that non-invasive somatosensory feedback via NMES not only  
417 enables higher subjective feeling of being in control (agency and confidence), but also  
418 leads to better actual control of the patient's BMI actions.

419  
420 **Agency covaries with BMI classifier.** We finally investigated whether agency has an  
421 impact on BMI efficiency and thus tested whether the sense of agency covaried with  
422 BMI classifier accuracy. We found that trials with agency versus trials without agency  
423 were associated with higher classifier accuracy when somatosensory feedback was  
424 modulated (Experiment 2;  $t(241) = 8.91$ , Cohen's  $d = 1.199$ ,  $p < 0.001$ ), as confirmed  
425 from analysis of data from Experiment 3 ( $t(446) = 6.256$ , Cohen's  $d = 0.601$ ,  $p < 0.001$ ).  
426 We found no statistically significant difference between trials with agency and trials  
427 without agency in classifier accuracy when visual feedback was modulated (Experiment  
428 1;  $t(153) = 0.690$ , Cohen's  $d = 0.111$ ,  $p = 0.49$ ). In addition, there was a significant  
429 correlation across all three experiments between BMI classifier accuracy and  
430 confidence (See Supplementary Table 1 for multiple regression analyses). Thus,  
431 agency and confidence were both directly related to the performance of the present BMI  
432 system, but only when somatosensory feedback was involved. In order to confirm the  
433 role of agency on BMI performance, while controlling for other potential factors, we  
434 compared the BMI performance between trials in which the BMI user reported high and  
435 low agency, within conditions at equivalent sensory feedback, that is V-/S+ and V+/S-  
436 from Experiment 3 (which resulted in a balanced and sufficient numbers of trials with  
437 "Yes" and "No" responses to Q1). As shown in Figure 5D, BMI accuracy varied as a  
438 function of subjective agency judgments, in conditions of equivalent sensory feedback.  
439 BMI accuracy was significantly higher in trials with high agency as compared to trials  
440 with low agency from 300 ms in the V-/S+ condition. The same pattern is visible in the  
441 V-/S+ condition, although the comparison was not significant (i.e., did not survive to  
442 correction for multiple comparisons). The same analysis run on confidence ratings (by  
443 sorting high and low confidence ratings by means of a median split) did not show any  
444 significant difference in BMI accuracy due to confidence at equivalent conditions of  
445 sensory feedback (see Supplementary Figure S6). These results suggest that the sense  
446 of agency, and not confidence (see Supplementary Table 1 for further analyses), has an  
447 effect on BMI accuracy beyond the prominent role of sensory feedback, and impacts  
448 BMI accuracy at a later time point. Since agency judgments and confidence ratings  
449 reflect two different processes of subjective experience, the present data suggest that

450 pre-reflexive, rather than post-decisional agency components more strongly affect the  
451 proficiency of a BMI decoder in M1.

452  
453

## 454 **Discussion**

455 By combining techniques from neurophysiology, neuroengineering, and VR with  
456 psychophysics of agency, we were able to study the sense of agency for actions  
457 enabled by a BMI-based intracortical neuroprosthesis and found that congruent sensory  
458 feedback boosted agency and confidence when controlling BMI actions. Moreover, we  
459 showed that human M1 processes not only motor and sensory information, but also  
460 different levels of congruency between sensory and motor signals and the resulting  
461 sense of agency. The present data are also of clinical relevance, because our NMES-  
462 based BMI approach, by providing congruent somatosensory feedback (without direct  
463 S1 stimulation) to a tetraplegic patient, improved the ability of the BMI classifier in  
464 decoding the patient's motor commands. Interestingly, such higher BMI proficiency was  
465 associated with a stronger sense of agency, suggesting that, beyond supporting close-  
466 loop systems and M1 feedback in general, somatosensory feedback and signals related  
467 to subjective aspects of motor control (i.e., agency) are important input for improving  
468 BMI proficiency. Quantifying subjective action-related mental states and including  
469 controlled motor and sensory feedback may therefore provide new levels of comfort and  
470 personalization and should be considered for the design of future BMIs.

471

472 The present data demonstrate that M1 activity contains information specifically linked to  
473 subjective aspects of motor control, in particular the sense of agency and confidence  
474 that our participant associated with his BMI actions. It is known that agency likely  
475 involves a network of multiple brain areas from which we did not record in the present  
476 study (e.g., posterior parietal cortex<sup>33</sup> and angular gyrus; anterior insula<sup>34,35</sup>;  
477 supplementary motor cortex<sup>36</sup>; premotor cortex<sup>37</sup>; for reviews see <sup>3,38</sup>). However, our  
478 findings – even if coming from a single tetraplegic patient - directly demonstrate that M1  
479 activity contains sufficient information to decode actions for which a human participant  
480 feels to be in control. The present BMI findings extend previous research that  
481 investigated the sense of agency for non-invasive BCI, as based on scalp



482 electroencephalography (EEG). They add important information about the underlying  
483 neural underpinnings based on M1 multiunit activity of the sense of agency in humans.  
484 In keeping with a prominent line of research on the role of visuo-motor (and visuo-  
485 tactile) cues in boosting or modulating body ownership for artificial and real limbs<sup>39–42</sup>,  
486 previous BCI studies also demonstrated that coherent visual feedback results in a  
487 higher sense of agency for BCI actions<sup>14</sup>. This effect is associated with stronger  
488 activations in a cortical-subcortical network, recruited during motor imagery used to  
489 control the BCI, consisting of posterior parietal cortex, insula, lateral occipital cortex,  
490 and basal ganglia<sup>13</sup>. Another study<sup>10</sup> further demonstrated that a stronger sense of  
491 agency for BCI-mediated actions is associated with stronger activity in sensorimotor  
492 areas during motor imagery based BCI. The present data on the sense of agency when  
493 using an intracortical BMI, although from a single, highly proficient BMI user (see  
494 below), demonstrate that this relationship can be tracked down even at the level of  
495 multi-unit activity from M1 neurons, and it is further associated with higher BMI  
496 proficiency.

497  
498 Moreover, the present findings offer a mechanistic explanation for the relationship  
499 between sensorimotor activity, sensory feedback and the resulting sense of agency, by  
500 showing that M1 activity before movement execution codes for the intended movement,  
501 while activity after movement execution encodes the sensory feedback associated with  
502 the implemented movement. By showing that somatosensory feedback in particular  
503 affects the performance of the BMI classifier, these analyses provide insights into the  
504 sensorimotor mechanisms of BMI proficiency. We note that this last finding was  
505 possible only due to the combination of a SCI lesion and the present intracortical BMI,  
506 which allowed us to decode efferent signals and manipulate afferent signals, not only as  
507 visual reproductions of body movements (via VR, as in previous studies), but also as  
508 physical movements of the real body (via NMES). In order to highlight the dynamic,  
509 multiscale brain mechanisms underlying the sense of agency in humans, future studies  
510 should combine insights that can be gained from invasive BMI - with ultra-high spatial  
511 resolution, but limited coverage in a handful of subjects – and non-invasive BCI – with  
512 limited resolution, but recording from the entire brain in larger subject samples.

513

514 Finally, our results can be of interest not only within the field of neuroprosthetics and its  
515 clinical application, but also for basic neuroscience as well as current ethical and legal  
516 debates about the subjective sense of agency and responsibility when applying  
517 neurotechnology solutions for human repair or enhancement<sup>38,43,44</sup>.

518  
519

### 520 **Limitations of the study**

521 Because of the uniqueness of the present experimental setup, generalization of the  
522 present findings to the general population should be done carefully. First, we tested a  
523 single participant, who is an extremely trained BMI user, who could have developed an  
524 extraordinary capacity of controlling his BMI system. This could have in turn impacted  
525 the associated sense of agency and the discovered links with BMI proficiency. Second,  
526 in order to enable movements of his upper limb, we used an NMES system that  
527 provides a series of somatosensory cues, which are only partially comparable to those  
528 associated with natural movements. For example, the intensity and temporal activation  
529 of somatosensory fibers as well as of the recruited motor fibers (antidromic) differs from  
530 sensorimotor activation during natural movements. We also note that although our  
531 participant suffered severe somatosensory loss (following damage at the C5-C6 level),  
532 he may have “learned” to associate some patterns of cutaneous sensations with the  
533 specific type of NMES stimulation used to enable specific movements. Indeed, outside  
534 of the experimental tasks described here, he was able to identify NMES-implemented  
535 movements even without seeing his arm. Finally, given the long-term spinal cord lesion  
536 suffered by this participant, we cannot exclude that some plastic changes have occurred  
537 in his motor representations in M1, his somatosensory representations in S1, or the  
538 connectivity between the two. There is still no consensus about plasticity following  
539 spinal cord injury, with some evidence of preserved network organization, some  
540 possible changes in grey matter density<sup>45,46</sup> or activation in the sensorimotor  
541 cortices<sup>47,48</sup>. It is also not clear how these results at the population level of SCI patients  
542 are predictive of changes at the single patient level. Thus, at the moment, it is not  
543 possible to exclude that some of the present results are idiosyncratic to this particular  
544 clinical case.

545

546  
547

548 **References**

- 549 1. Blakemore, S. J., Wolpert, D. M. & Frith, C. D. Abnormalities in the awareness of  
550 action. *Trends Cogn. Sci.* **6**, 237–242 (2002).
- 551 2. Jeannerod, M. *Motor cognition : what actions tell the self.* (Oxford University  
552 Press, 2006).
- 553 3. Haggard, P. Sense of agency in the human brain. *Nat. Rev. Neurosci.* **18**, 196–  
554 207 (2017).
- 555 4. Hochberg, L. R. *et al.* Reach and grasp by people with tetraplegia using a neurally  
556 controlled robotic arm. *Nature* **485**, 372–375 (2012).
- 557 5. Collinger, J. L. *et al.* High-performance neuroprosthetic control by an individual  
558 with tetraplegia. *Lancet* **381**, 557–564 (2013).
- 559 6. Bouton, C. E. *et al.* Restoring cortical control of functional movement in a human  
560 with quadriplegia. *Nature* **533**, 247–250 (2016).
- 561 7. Ajiboye, A. B. *et al.* Restoration of reaching and grasping movements through  
562 brain-controlled muscle stimulation in a person with tetraplegia: a proof-of-concept  
563 demonstration. *Lancet* **389**, 1821–1830 (2017).
- 564 8. Lebedev, M. A. & Nicolelis, M. A. L. Brain-Machine Interfaces: From Basic  
565 Science to Neuroprostheses and Neurorehabilitation. *Physiol. Rev.* **97**, 767–837  
566 (2017).
- 567 9. Donoghue, J. P. Connecting cortex to machines: recent advances in brain  
568 interfaces. *Nat. Neurosci.* **5**, 1085–1088 (2002).
- 569 10. Nierula, B. *et al.* Agency and responsibility over virtual movements controlled  
570 through different paradigms of brain–computer interface. *J. Physiol.* **0**, 1–16  
571 (2019).
- 572 11. Nierula, B. & Sanchez-Vives, M. V. Can BCI Paradigms Induce Feelings of  
573 Agency and Responsibility Over Movements? in (2019). doi:10.1007/978-3-030-  
574 05668-1\_10.
- 575 12. Sato, A. & Yasuda, A. Illusion of sense of self-agency: Discrepancy between the  
576 predicted and actual sensory consequences of actions modulates the sense of  
577 self-agency, but not the sense of self-ownership. *Cognition* **94**, 241–255 (2005).
- 578 13. Marchesotti, S. *et al.* Cortical and subcortical mechanisms of brain-machine  
579 interfaces. *Hum. Brain Mapp.* **38**, 2971–2989 (2017).
- 580 14. Evans, N., Gale, S., Schurger, A. & Blanke, O. Visual Feedback Dominates the  
581 Sense of Agency for Brain-Machine Actions. *PLoS One* **10**, e0130019 (2015).
- 582 15. Knoblich, G. & Sebanz, N. Agency in the face of error. *Trends Cogn. Sci.* **9**, 259–  
583 261 (2005).
- 584 16. Tsakiris, M., Prabhu, G. & Haggard, P. Having a body versus moving your body:  
585 How agency structures body-ownership. *Conscious. Cogn.* **15**, 423–432 (2006).
- 586 17. Scott, S. H., Cluff, T., Lowrey, C. R. & Takei, T. Feedback control during voluntary  
587 motor actions. *Curr. Opin. Neurobiol.* **33**, 85–94 (2015).

- 588 18. Shokur, S. *et al.* Expanding the primate body schema in sensorimotor cortex by  
589 virtual touches of an avatar. *Proc. Natl. Acad. Sci.* **110**, 15121–15126 (2013).
- 590 19. Hatsopoulos, N. G. & Suminski, A. J. Sensing with the motor cortex. *Neuron* **72**,  
591 477–487 (2011).
- 592 20. Hatsopoulos, N. G., Xu, Q. & Amit, Y. Encoding of movement fragments in the  
593 motor cortex. *J. Neurosci.* **27**, 5105–14 (2007).
- 594 21. Suminski, A. J., Tkach, D. C., Fagg, A. H. & Hatsopoulos, N. G. Incorporating  
595 Feedback from Multiple Sensory Modalities Enhances Brain-Machine Interface  
596 Control. *J. Neurosci.* **30**, 16777–16787 (2010).
- 597 22. Tkach, D., Reimer, J. & Hatsopoulos, N. G. Congruent activity during action and  
598 action observation in motor cortex. *J. Neurosci.* **27**, 13241–50 (2007).
- 599 23. Churchland, M. M. & Shenoy, K. V. Temporal Complexity and Heterogeneity of  
600 Single-Neuron Activity in Premotor and Motor Cortex. *J. Neurophysiol.* **97**, 4235–  
601 4257 (2007).
- 602 24. Schwartz, A. B. Movement: How the Brain Communicates with the World. *Cell*  
603 **164**, 1122–1135 (2016).
- 604 25. O’Doherty, J. E. *et al.* Active tactile exploration using a brain–machine–brain  
605 interface. *Nature* **479**, 228–231 (2011).
- 606 26. Stepniewska, I., Preuss, T. M. & Kaas, J. H. Architectonics, somatotopic  
607 organization, and ipsilateral cortical connections of the primary motor area (M1) of  
608 owl monkeys. *J. Comp. Neurol.* **330**, (1993).
- 609 27. Eickhoff, S. B. *et al.* Anatomical and functional connectivity of cytoarchitectonic  
610 areas within the human parietal operculum. *J. Neurosci.* **30**, (2010).
- 611 28. Fetz, E. E., Finocchio, D. V., Baker, M. A. & Soso, M. J. Sensory and motor  
612 responses of precentral cortex cells during comparable passive and active joint  
613 movements. *J. Neurophysiol.* **43**, (1980).
- 614 29. Hochberg, L. R. *et al.* Neuronal ensemble control of prosthetic devices by a  
615 human with tetraplegia. *Nature* **442**, 164–171 (2006).
- 616 30. Tabot, G. A. *et al.* Restoring the sense of touch with a prosthetic hand through a  
617 brain interface. *Proc. Natl. Acad. Sci. U. S. A.* **110**, 18279–84 (2013).
- 618 31. Flesher, S. N. *et al.* Intracortical microstimulation of human somatosensory cortex.  
619 *Sci. Transl. Med.* **8**, 361ra141 LP-361ra141 (2016).
- 620 32. Bensmaia, S. J. & Miller, L. E. Restoring sensorimotor function through  
621 intracortical interfaces: progress and looming challenges. *Nat. Rev. Neurosci.* **15**,  
622 313–325 (2014).
- 623 33. Desmurget, M. *et al.* Movement intention after parietal cortex stimulation in  
624 humans. *Science* **324**, 811–3 (2009).
- 625 34. Farrer, C. & Frith, C. D. Experiencing Oneself vs Another Person as Being the  
626 Cause of an Action: The Neural Correlates of the Experience of Agency.  
627 *Neuroimage* **15**, 596–603 (2002).

- 628 35. Chambon, V., Wenke, D., Fleming, S. M., Prinz, W. & Haggard, P. An online  
629 neural substrate for sense of agency. *Cereb. Cortex* **23**, 1031–1037 (2013).
- 630 36. Fried, I., Mukamel, R. & Kreiman, G. Internally Generated Preactivation of Single  
631 Neurons in Human Medial Frontal Cortex Predicts Volition. *Neuron* **69**, 548–562  
632 (2011).
- 633 37. Fornia, L. *et al.* Direct electrical stimulation of the premotor cortex shuts down  
634 awareness of voluntary actions. *Nat. Commun.* **11**, 1–11 (2020).
- 635 38. Sperduti, M., Delaveau, P., Fossati, P. & Nadel, J. Different brain structures  
636 related to self- and external-agency attribution: A brief review and meta-analysis.  
637 *Brain Struct. Funct.* **216**, 151–157 (2011).
- 638 39. Blanke, O., Slater, M. & Serino, A. Behavioral, Neural, and Computational  
639 Principles of Bodily Self-Consciousness. *Neuron* **88**, 145–166 (2015).
- 640 40. Makin, T. R., Holmes, N. P. & Ehrsson, H. H. On the other hand: Dummy hands  
641 and peripersonal space. *Behav. Brain Res.* **191**, 1–10 (2008).
- 642 41. Rognini, G. *et al.* Multisensory bionic limb to achieve prosthesis embodiment and  
643 reduce distorted phantom limb perceptions. *J. Neurol. Neurosurg. Psychiatry* **90**,  
644 833–836 (2019).
- 645 42. Sanchez-Vives, M. V., Spanlang, B., Frisoli, A., Bergamasco, M. & Slater, M.  
646 Virtual hand illusion induced by visuomotor correlations. *PLoS One* **5**, e10381  
647 (2010).
- 648 43. Yuste, R. *et al.* Four ethical priorities for neurotechnologies and AI. *Nature* **551**,  
649 159–163 (2017).
- 650 44. Fried, I., Haggard, P., He, B. J. & Schurger, A. Volition and Action in the Human  
651 Brain: Processes, Pathologies, and Reasons. *J. Neurosci.* **37**, 10842–10847  
652 (2017).
- 653 45. Wang, W. *et al.* Specific Brain Morphometric Changes in Spinal Cord Injury: A  
654 Voxel-Based Meta-Analysis of White and Gray Matter Volume. *J. Neurotrauma*  
655 **36**, (2019).
- 656 46. Melo, M. C., Macedo, D. R. & Soares, A. B. Divergent Findings in Brain  
657 Reorganization After Spinal Cord Injury: A Review. *Journal of Neuroimaging* vol.  
658 30 (2020).
- 659 47. Freund, P. *et al.* MRI investigation of the sensorimotor cortex and the  
660 corticospinal tract after acute spinal cord injury: A prospective longitudinal study.  
661 *Lancet Neurol.* **12**, (2013).
- 662 48. Henderson, L. A., Gustin, S. M., Macey, P. M., Wrigley, P. J. & Siddall, P. J.  
663 Functional reorganization of the brain in humans following spinal cord injury:  
664 Evidence for underlying changes in cortical anatomy. *J. Neurosci.* **31**, (2011).
- 665 49. Mallat, S. *A Wavelet Tour of Signal Processing. A Wavelet Tour of Signal*  
666 *Processing* (2009). doi:10.1016/B978-0-12-374370-1.X0001-8.
- 667 50. Humber, C., Ito, K. & Bouton, C. Nonsmooth Formulation of the Support Vector  
668 Machine for a Neural Decoding Problem. *arXiv* (2010).

- 669 51. Colachis, S. C. *et al.* Dexterous control of seven functional hand movements  
670 using cortically-controlled transcutaneous muscle stimulation in a person with  
671 tetraplegia. *Front. Neurosci.* **12**, 1–14 (2018).
- 672 52. Colachis, S. C. I. Optimizing the Brain-Computer Interface for Spinal Cord Injury  
673 Rehabilitation. (2018).
- 674 53. Zhang, M. *et al.* Extracting wavelet based neural features from human intracortical  
675 recordings for neuroprosthetics applications. *Bioelectron. Med.* **4**, 11 (2018).
- 676 54. Quiroga, R. Q., Nadasdy, Z. & Ben-Shaul, Y. Unsupervised Spike Detection and  
677 Sorting with Wavelets and Superparamagnetic Clustering. *Neural Comput.* **16**,  
678 1661–1687 (2004).
- 679 55. Hoerl, A. E. & Kennard, R. W. Ridge Regression: Biased Estimation for  
680 Nonorthogonal Problems. *Technometrics* **12**, 55–67 (1970).
- 681 56. Kuhn, M. R Package: caret, Ver. 6.0-80. *CRAN* (2018).
- 682 57. Maris, E. & Oostenveld, R. Nonparametric statistical testing of EEG- and MEG-  
683 data. *J. Neurosci. Methods* **164**, 177–190 (2007).
- 684
- 685

686 **Acknowledgments**

687 The authors thank Ian for his dedication to the study and insightful conversations.

688 AS is supported by the Swiss National Science Foundation (grant (PP00P3\_163951 /  
689 1), OB is supported by the Swiss National Science Foundation and the Bertarelli  
690 Foundation. MB is supported by the Craig H. Neilsen Foundation (Grant  
691 number: 651289) and State of Ohio Research Incentive Third Frontier Fund. The  
692 funders had no role in study design, data collection and analysis, decision to publish or  
693 preparation of the manuscript.

694

695 **Author contributions** AS: Conceptualization, Formal Analysis, Methodology, Writing;  
696 *MB*: Methodology, Investigation, Project Administration, Review & Editing; TB: Data  
697 curation, Formal analysis, Software, Visualization, Review & editing; SC: Methodology,  
698 Data Curation, Formal analysis, Investigation, Software; MS: Formal analysis,  
699 Investigation, Visualization, Review & editing; CD, KE: Investigation, Data collection PG:  
700 Methodology, Review & Editing; GS: Methodology, Software and Hardware  
701 development; NA: Methodology, Review & editing; PO: Investigation, Software and  
702 Hardware development, DF: Investigation, Software and Hardware development, PS:  
703 Methodology, Review & editing; NF: Formal analysis, Methodology, Visualization,  
704 Review & editing; AR: Funding acquisition, Resources, Supervision, Review & editing;  
705 OB: Conceptualization, Funding acquisition, Methodology, Supervision, Writing.

706

707 **Competing interests:** AS, MS, TB, NF, PS, and OB declare no competing interests.  
708 CD, KE, PG, GS, NA, and DF hold patents for the BMI system.

709



710 **Figure legends**

711

712 **Figure 1. Experimental setup.** A. Events during trials. One (out of four possible  
713 movements) was cued, following a “Go” signal to initiate the movement. The BMI  
714 classifier decoded the movement from M1 activity and sensory feedback was given. The  
715 patient answered two questions: Q1. “Are you the one who generated the movement?”,  
716 by saying “Yes” or “No”; and Q2. “How confident are you?”, by indicating a number  
717 ranging from 0 (absolutely unsure) to 100 (absolutely sure). B: Example of sensory  
718 feedback for one type of movement. The chosen movement was realized as a visual  
719 feedback, via virtual reality (VR – Experiment 1), as a somatosensory feedback, via  
720 NEMS (Experiment 2) or both (Experiment 3). In different congruency conditions, either  
721 the cued and correctly decoded movement (Congruent) or the opposite movement  
722 (Incongruent) was realized for the different modalities. The location of the electrodes  
723 array in the M1, with respect to the pattern of activity for upper limb attempted  
724 movement from fMRI is also shown (from <sup>6</sup>).

725

726 **Figure 2. Agency judgements and confidence depends on sensory feedback.** A.  
727 Proportion of “Yes” and “No” answers (Q1) to congruent and incongruent trials for the  
728 visual (Experiment 1) somatosensory (Experiment 2) and the combination of the two  
729 modalities (Experiment 3). B-C-D: Confidence about agency judgments. Distribution of  
730 Q2 responses as a function of the congruency of visual (B), somatosensory (C) or both  
731 (D) sensory feedback.

732

733 **Figure 3. M1 activity depends on sensory feedback.** Sensory feedback as encoded  
734 by Local field potentials (LFP; left panel) and Multiunit firing rates (MU; right panel). LFP  
735 and MU modulation for congruent and incongruent visual (Experiment 1) and  
736 somatosensory (Experiment 2) feedback (A) and for the combination of the two  
737 (Experiment 3, B). Colored lines represent averaged signal across all channels (shaded  
738 areas indicate SEMs); black lines report the time-related k-values of the multivariate  
739 decoder distinguishing between congruent and incongruent feedback; the underlying  
740 thick segments indicate k-values significantly higher than chance level from cluster-  
741 based permutation analyses.

742

743 **Figure 4. Sense of agency in M1.** Sense of agency as coded by LFP (left) and Multi-  
744 unit firing rates (right). A. Left and right panels respectively show averaged LFP and  
745 Multi-unit modulation for high (green) and no (grey) agency response to Q1 (shaded  
746 areas indicate SEMs); black lines report the time-related k-values of the multivariate  
747 decoder distinguishing the two conditions; the underlying thick segments indicate k-  
748 values significantly higher than chance level from cluster-based permutation analyses.  
749 B: Results of the decoder discriminating between high vs. low orthogonalized agency  
750 scores from LFP (left) and MU (right) after regressing out for the effects of the  
751 congruency of sensory feedback and type of movements.

752

753 **Figure 5. Performance of BMI classifier as a function of sensory feedback and**  
754 **sense of agency.** A-B-C. The left panels (A, B, C) show the modulation in time of the  
755 performance of the BMI classifier for the 4 types of movements indicated for the cued  
756 movement (filled line) and the opposite (dashed line), as a function of feedback (i.e.  
757 black dots indicate time points with significant difference). The right panels show the  
758 area under the curve taken as an index of global performance of the BMI. The  
759 performance of the BMI classifier does vary not as a function of visual feedback  
760 (Experiment 1, A), but it is significantly better when somatosensory feedback is  
761 congruent both in Experiment 2 (B) and in Experiment 3 (C). D. BMI accuracy in time as  
762 a function of sense of agency. Blue/red curves represent the BMI classifier output for  
763 the cued movement as a function of agency judgements (Q1: 1=high agency; 0=low  
764 agency) in conditions of equal sensory feedback.

765

766

767 **Figure 6. Somatosensory feedback changes firing rates of M1 neurons. A-B.**  
768 Euclidean distance in time between trials with same motor intention and opposite  
769 feedback (red), same feedback and opposite intention (blue), or opposite congruent  
770 feedback and intention (green), for experiment 1 (A) and 2 (B). In Experiment 1, neural  
771 activity diverged as a function of motor intention before the movement, as shown by the  
772 increase in Euclidean distances between the green and blue curves. In Experiment 2,  
773 neural activity diverged as function of sensory feedback after NMES activation. **C-D.**

774 Multidimensional scaling of neural activity before (-650/150 ms; C) and after (0/500 ms;  
775 D) sensory feedback. The plots show a 2D dimensionality reduction of population  
776 activity in the target period, in order to represent it on a plane. As in a principal  
777 component analysis, Dimensions 1 and 2 can be seen as the two abstract coordinates  
778 explaining most variance in the data. Movements are separated by classes of hand  
779 (open/close; right) and thumb (extension / flexion; left) movements.

780

781

782

783

784

## 785 **Materials and Methods**

### 786 **Participant**

787 The participant in this study was enrolled in a pilot clinical trial (NCT01997125) of a  
788 custom neural bridging system (Battelle Memorial Institute) to reanimate paralyzed  
789 upper limbs after C4-6 spinal cord injury. The system consisted of a Neuroport data  
790 acquisition system (Blackrock Micro, Salt Lake, Utah), custom signal processing and  
791 decoding algorithms (Battelle), and a NeuroLife Neuromuscular Stimulation System  
792 (Battelle). The trial received investigational device exemption (IDE) approval by the US  
793 Food and Drug Administration and Institutional Review Board approval through the Ohio  
794 State University (Columbus, Ohio). The study conformed to institutional research  
795 requirements for the conduct of human subjects. The site of the experiments was the  
796 Ohio State University NeuroRehabLab (Bockbrader, PI) and data was analyzed at Ohio  
797 State (Columbus, Ohio) and École polytechnique fédérale de Lausanne (EPFL,  
798 Switzerland). The participant provided informed consent at the time of enrollment and  
799 also provided written permission for photographs and videos.

800 The study participant was a 22 year-old male at the time of study enrollment. He had  
801 complete C5 ASIA A, non-spastic tetraparesis from cervical spinal cord injury  
802 associated with a diving accident 3 years prior. On neurological exam, he had full motor  
803 function bilaterally for C5 level muscles (e.g., biceps and shoulder girdle muscles), but  
804 no motor function below the C6 level. He had 1/5 strength on the right and 2/5 strength  
805 on the left for wrist extension (C6 level) on manual muscle testing. His sensory level  
806 was C6 on the left and C5 on the right, although he had sensation for pressure on his  
807 right thumb. He had preserved proprioception for shoulder, elbow and wrist joint  
808 position, but was at chance level for distinguishing digit joint positions  
809 (flexion/neutral/extension) for the thumb and fingers. He had mild finger flexor  
810 contractures bilaterally, limiting finger extension at the proximal and distal  
811 interphalangeal joints of digits 2-5.

812 He was implanted with a 4.4 x 4.2mm intracortical silicon Neuroport microelectrode  
813 array (Blackrock Microsystems) in the dominant hand/arm area of his motor cortex on  
814 4/22/2014, as previously described<sup>6</sup>. The implant site was determined by preoperative  
815 functional neuroimaging obtained while the participant visualized movements of his right

816 hand and forearm. He began using cortically-controlled transcutaneous neuromuscular  
817 electrical stimulation (NMES) on his right forearm on 5/23/14. Data for this study was  
818 collected over 13 sessions (45 hours) from 11/16/2016 - 2/20/2017, corresponding to  
819 post-implant days 939-1035. One session with visual and NMES feedback was used for  
820 practice (5 blocks of 32 trials on post-implant day 939). At the time of data collection,  
821 the participant was an expert brain-machine interface (BMI) user with over 800 hours of  
822 study participation.

823 The participant underwent cognitive testing approximately one year after Utah array  
824 implantation (January – July, 2015). He scored with superior verbal abilities, attention,  
825 and working memory (ranging between 92<sup>nd</sup> - 99<sup>th</sup> percentile for his age).

826

### 827 **Cortical Signal Acquisition and Classification**

828 Neural data (96 channels) were acquired from the left motor cortex Utah array through  
829 the Neuroport data acquisition system (Blackrock Micro). Raw data were processed  
830 using analog hardware with 0.3Hz 1<sup>st</sup> order high-pass and 7.5kHz 3<sup>rd</sup> order Butterworth  
831 low-pass filters, then digitized at 30,000 Hz. Data were divided into 100ms bins and  
832 passed into Matlab (version 2014b), where signal artifact was removed by blanking over  
833 3.5ms around artifacts (defined as signal amplitude >500 $\mu$ V at the same time on 4 of 12  
834 randomly-selected channels). Signals were decomposed into mean wavelet power  
835 (MWP) using the 'db4' wavelet over 100ms<sup>49</sup>. Coefficients within the multiunit frequency  
836 bands (234–3,750Hz, coefficients of scales 3, 4, 5, 6) were averaged across the 100ms  
837 window and normalized by channel (by subtracting the mean and dividing by the  
838 standard deviation of each channel and scale, respectively). Normalized coefficients for  
839 each channel were averaged across scales 3-6, creating 96 MWP values (one for each  
840 channel) per each 100ms. MWP values were fed as features into a real-time, nonlinear  
841 support vector machine (SVM) classifier<sup>50</sup> with five classes (hand open, hand closed,  
842 thumb extension, thumb flexion, and rest). Classifier activation values were computed  
843 for each 100ms bin and ranged from -1 to 1. Classifier output represented the  
844 movement pattern (hand open, hand closed, thumb extension, thumb flexion) with the  
845 highest activation greater than threshold (zero). If no movement classes had activation

846 greater than zero, the classifier was in the “rest” state. If multiple output classes  
847 exceeded threshold, only the one with the highest score was used to provide feedback.  
848 Signal quality was stable<sup>51</sup> during the interval of data collection; but represented about a  
849 30% decline in MWP normalized to post-implant 87<sup>52</sup>. (See below for single unit  
850 statistics.) Average impedance was approximately 200 k $\Omega$ , a decline of 40% of its initial  
851 value. Average signal-to-noise was approximately 17.5dB, a decrease of about 10% of  
852 its initial value<sup>53</sup>. Most of the decline in signal quality occurred in the first 400 days post-  
853 implantation.

854

### 855 **Classifier Training and Neurally Controlled Hand Movements**

856 Before each session, the SVM classifier was trained in an adaptive manner over 5  
857 blocks. Each block consisted of 3 repetitions of 4 movements (hand open, hand closed,  
858 thumb extension, thumb flexion) presented in a random order. Movements were cued  
859 for 3-4s (4-5s inter-cue interval) using a small, animated hand in the corner of the video  
860 display. Feedback was given with both NMES and the feedback hand on the video  
861 screen. During the first training block, scripted feedback was provided simultaneously  
862 with the cued movements. In subsequent blocks, appropriate movements were  
863 activated when an output class for a given movement exceeded threshold (>0).  
864 Training took approximately 10-15 minutes per session.

865

### 866 **Neuromuscular Electrical Stimulation**

867 The NMES system was used to evoke hand and finger movements by stimulating  
868 forearm muscles. The system consisted of a multi-channel stimulator and a flexible,  
869 130-electrode, circumferential forearm cuff. Coated copper electrodes with hydrogel  
870 interfaces (Axelgaard, Fallbrook, CA) were 12mm in diameter, spaced at regular  
871 intervals in an array (22mm longitudinally X 15mm transversely), and delivered current  
872 in monophasic, rectangular pulses at 50Hz (pulse width 500 $\mu$ s, amplitude 0-20mA).  
873 Desired hand/finger movements were calibrated at the beginning of each session by  
874 determining/confirming the intensity and pattern of electrodes required to stimulate  
875 intended movements. This took 5-10 minutes per session.

876 During the experiment, the participant's view of NMES-evoked movements was  
877 obscured from view by the video display. During Experiment 1, non-informative NMES  
878 feedback was given (current at an intensity equivalent to what was used for movement  
879 calibration patterns, but that did not evoke movement). During Experiments 2 and 3,  
880 NMES feedback was provided that evoked hand and finger movements.

881

### 882 **Virtual Reality Animation**

883 A non-immersive virtual reality system (i.e. without a head-mounted display or head-  
884 tracking) was used to provide visual feedback. This was done in order to adopt a  
885 previous setup that the participant was already familiar with to the present experiments  
886 and also facilitated the calibration procedure to train the BMI classifier. A physics-based  
887 animated hand was used to provide visual feedback of classifier activation. During  
888 training, two animated hands were displayed, a small cue hand at the bottom left and a  
889 larger centrally-placed feedback hand (Figure 1 main text). During the experiment, the  
890 display was oriented over the participant's forearm, a single, centrally-placed feedback  
891 hand was displayed to match the size and location of the participant's right hand (the  
892 cue hand was not displayed). During Experiments 1 and 3, feedback was provided  
893 using the virtual hand. During Experiment 2, non-informative visual feedback was given  
894 (the feedback hand remained in a neutral, rest position).

895

### 896 **Feedback Congruency**

897 In half of the trials across Experiments, the visual and/or somatosensory feedback was  
898 covertly manipulated to be incongruent with the cue. In incongruent trials, when the  
899 participant correctly activated the classifier associated with the cue, he received  
900 feedback opposite to the cue (i.e., hand closed for "hand open", thumb extension for  
901 "thumb flex", etc.). In congruent trials, he received feedback consistent with the cue  
902 (i.e., hand open for "hand open", thumb flexion for "thumb flex", etc.).

903

### 904 **Agency Assessment**

905 All experimental trials began with a verbal cue ("hand open", "hand closed", "thumb  
906 extend", "thumb flex"), followed by a 2 second delay, then a verbal cue ("go"). During  
907 the next 4s, the participant was given feedback based on classifier activation levels, and

908 then was told to “stop”). Over the next 5-5.5s, the participant reported whether he felt in  
909 control of the movement (“yes” or “no”) and his degree of certainty (0-100). The next  
910 trial began at the end of this 5-5.5s interval. There were 32 trials per block in  
911 Experiments 1 and 2 and 26 trials per block in Experiment 3.

912

### 913 **Trial Selection and Time-locking**

914 To ensure that the participant was successfully activating the classifier for the cued  
915 movement, and the signal can be meaningfully time-locked to movement onset, we  
916 applied the following selection criteria on the trials. We consider it as a correct imagined  
917 movement when the participant is able to maintain the classifier of the cued movement  
918 above the threshold for at least 600 ms (6 classifier output bins). We retain trials in  
919 which at least one correct movement happens between the GO cue and 1.5 seconds  
920 before the STOP cue. Epochs are then constructed by time-locking every trial with  
921 respect to the onset of such imagined movements. In case several correct movements  
922 occurred during the same trial, the time-locking is relative to the first movement.  
923 Furthermore, we excluded 128 trials from the session on which the participant  
924 systematically reported problems with controlling the BMI system and absent subjective  
925 agency. Globally, we retained 846 out of 1408 trials (60%).

926 Note that, since we define the onset as the beginning of the 100 ms bin of neural activity  
927 that is fed to the classifier, and around 50 ms are required to compute the output, the  
928 corresponding feedback is received about 150 ms after the onset of the imagined  
929 movement.

930

### 931 **Experiment 1: Agency Assessment with Virtual Hand Feedback and Non-** 932 **informative NMES**

933 Twelve blocks of 32 trials were collected on post-implant days 953 (4 blocks), 988 (4  
934 blocks), and 1035 (4 blocks). In each trial, the participant received a verbal cue to  
935 perform a movement (“hand open”, “hand closed”, “thumb extend”, “thumb flex”). When  
936 a classifier crossed threshold during the 4 second feedback window, feedback was  
937 given by showing movement of the virtual hand and by activating non-informative NMES  
938 (radial wrist electrode activation that did not elicit movement, did not vary from trial to  
939 trial, and that the participant could feel and distinguish from real NMES feedback).



940 Feedback on half of the trials was randomly selected to be incongruent with the cue. His  
941 subjective sense of agency and level of certainty were recorded for each trial.

942 A total of 384 trials were collected across three days. After removing trials where the  
943 cued action could not be correctly decoded and the session on post-implant day 1035  
944 (see trial selection paragraph), 83 congruent and 72 incongruent trials remained for  
945 behavioral and neural activity analysis.

946

### 947 **Experiment 2: Agency Assessment with NMES Feedback and Non-informative** 948 **Virtual Hand**

949 Twelve blocks of 32 trials were collected on post-implant days 941 (5 blocks), 960 (3  
950 blocks), and 967 (4 blocks). In each trial, the participant received a verbal cue to  
951 perform a movement (“hand open”, “hand closed”, “thumb extend”, “thumb flex”). When  
952 a classifier crossed threshold during the 4 second feedback window, feedback was  
953 given by activating movement of the participant’s hand and wrist through NMES and  
954 showing non-informative visual feedback (non-moving hand). The participant could not  
955 see his own hand/wrist, but could distinguish his hand state based what the stimulation  
956 patterns felt like to him. Feedback on half of the trials was randomly selected to be  
957 incongruent with the cue. His subjective sense of agency and level of certainty were  
958 recorded for each trial.

959 A total of 384 trials were collected across three days. After removing trials where the  
960 participant did not respond correctly by activating the classifier associated with the cue,  
961 154 congruent and 89 incongruent trials remained for behavioral and neural activity  
962 analysis.

963

### 964 **Experiment 3: Agency Assessment with Virtual Hand and NMES Feedback**

965 Twenty blocks of 32 trials were collected on post-implant days 993 (3 blocks), 990 (5  
966 blocks), 1007 (4 blocks), 1014 (3 blocks), and 1021 (5 blocks). In each trial, the  
967 participant received a verbal cue to perform a movement (“hand open”, “hand closed”,  
968 “thumb extend”, “thumb flex”). When a classifier crossed threshold during the 4 second  
969 feedback window, feedback was given by activating movement of the participant’s hand  
970 and wrist through NMES and showing movement of the virtual hand. The participant  
971 could not see his own hand/wrist, but could distinguish his hand state based what the

972 stimulation patterns felt like to him. Congruency with respect to the cue was  
973 manipulated independently in the visual and somatosensory modalities such that 25%  
974 of the trials were each: congruent for both visual and NMES feedback, incongruent for  
975 both visual and NMES feedback, congruent for visual but incongruent for NMES  
976 feedback, congruent for NMES but incongruent for visual feedback. His subjective  
977 sense of agency and level of certainty were recorded for each trial.

978 A total of 520 trials were collected across five days. After removing trials where the  
979 participant did not respond correctly by activating the classifier associated with the cue,  
980 the number of trials that remained for behavioral and neural activity analysis were: 117  
981 congruent for both visual and NMES feedback, 103 incongruent for both visual and  
982 NMES feedback, 101 congruent for visual and incongruent for NMES feedback, and  
983 127 congruent for NMES and incongruent for visual feedback.

984

### 985 **Firing Rate Calculation and Single Unit Analyses**

986 Single units were identified through offline data processing. For each block, raw voltage  
987 recordings at each channel were processed in a series of steps. First, FES stimulation  
988 artifact was removed using a 500 $\mu$ V threshold and 3.5ms artifact removal time window.  
989 The removed window was replaced with an interpolated segment to retain temporal  
990 information. Then, the raw signal with FES artifact removed was processed with a 300-  
991 3000Hz bandpass filter. The filtered data was fed into an automated spike detection and  
992 sorting algorithm, wave\_clus<sup>54</sup> using the default optimization settings. A threshold was  
993 set to four times the standard deviation of the noise and used to detect spike locations.  
994 A wavelet decomposition was performed on the spikes to extract features and a  
995 superparamagnetic clustering algorithm was used to cluster the spikes into groups,  
996 representative of individual single units. The superparamagnetic clustering algorithm  
997 was used to eliminate spikes that were considered noise to ensure only single units  
998 were analyzed. As spike sorting was not performed before data collection, there was no  
999 way to match single units across days. Additionally, the number of single units detected  
1000 at a given channel fluctuated between days, possibly due to micro-movement of the  
1001 array and brain state changes. For this reason, all single units detected at a given  
1002 channel were considered the same and pooled at the single channel level as multiunit  
1003 activity in subsequent analysis.

1004

### 1005 **Offline neural decoding**

1006 Sensory feedback congruency and subjective ratings (Q1 and Q2) were decoded offline  
1007 both from LFPs and from multiunit activity. For LFP analysis, the signal amplitude for  
1008 each channel was downsampled to 500 Hz, band-passed between 0.1 and 12 Hz with  
1009 an IIR filter and smoothed using sliding averaging windows of 250 ms. Following  
1010 multiunit spike times calculation (see above), multiunit firing rate was estimated at 20 Hz  
1011 over a 250 ms sliding window.

1012 We fed each channel's signal amplitude (LFP) or firing rate (multiunit) as predictors to a  
1013 penalized linear decoder based on ridge regressions<sup>55</sup>. A separate model was trained to  
1014 decode congruency (Q1) or confidence (Q2) on each signal timepoint, with a sampling  
1015 rate of 20 and 500 Hz for multiunit and LFPs respectively. Decoding performance was  
1016 evaluated by computing and averaging Cohen's  $k$  (logistic regression; Q1) or  $R^2$  (linear  
1017 regression; Q2) values over 10 independent 10-fold cross validation runs. The  
1018 regression was performed through the "train" function of the R "caret" package<sup>56</sup>. To  
1019 evaluate the statistical significance of the decoding, we generated a null decoding  
1020 performance distribution by applying the same decoding methods on the data after  
1021 randomly shuffling Q1 and Q2 values. 1000 permutations were generated, and the  
1022 decoding performance was evaluated for each of them. Then, a t-value was assigned to  
1023 every time-point both in real and permuted data, by comparing its decoding  
1024 performance to the null distribution of permuted data. Finally, the t-values were used to  
1025 define significant decoding time windows based on a cluster-based permutation test on  
1026 each epoch's largest cluster<sup>57</sup>. After checking that the t-value threshold used to define  
1027 clusters was not significantly affecting the results, its value was set at 2.

1028

### 1029 **Computation of distance between neural activity patterns**

1030 Since the neural activity recorded by the microelectrode array can change significantly  
1031 between experimental sessions (i.e., days of recording) spanned by our analysis,  
1032 Euclidean distances per each pair of conditions were computed separately within each  
1033 day of recording and then averaged to obtain the final results. Confidence intervals were  
1034 obtained through a bootstrapping technique, again applied within sessions. For each

1035 session and condition, we extracted n random trials with replacement, where n is the  
1036 number of trials for that condition/session, and the final Euclidean distance was  
1037 obtained by averaging across sessions as described above. The procedure was  
1038 repeated 100 times, and 95 % confidence intervals were obtained as 1.96 times the  
1039 standard deviation of the surrogated distribution obtained as explained here.

1040

### 1041 **Multidimensional scaling**

1042 In order to graphically represent the spatio-temporal patterns of neural activity, we  
1043 performed a multidimensional scaling (MATLAB function mds) on correlation distances  
1044 computed between spatio-temporal patterns of neural activity. Also, in this case, to  
1045 avoid including sources of variances due to the change in signal between experimental  
1046 sessions, the procedure was run within experimental sessions. In order to obtain  
1047 correlation distances between trials we started by concatenating, for each trial, data  
1048 from all channels and timepoints within the selected temporal window. Then, we  
1049 computed the correlation coefficient of the resulting vector with the equivalent vector  
1050 from all other trials within the same session and subtracted the obtained values to 1 to  
1051 obtain values of the correlation distance. The first two dimensions of the  
1052 multidimensional scaling were then aligned across sessions via the Procrustes analysis  
1053 (MATLAB function Procrustes), using the means by conditions (combinations of  
1054 movement/somatosensory feedback) in the first session as a reference.

1055

1056

### 1057 **Data availability statement**

1058

1059 Behavioral data and processed data necessary to reproduce the figures in the main text  
1060 can be found in the OSF repository accessible at:

1061 [https://osf.io/7rma5/?view\\_only=9928bd8e32a748828f7ecfdbeb1f8baa](https://osf.io/7rma5/?view_only=9928bd8e32a748828f7ecfdbeb1f8baa).

1062 Neural data and code for BMI control can be made available to qualified individuals for  
1063 collaboration via a written agreement between Battelle Memorial Institute and the  
1064 requester's affiliated institution. Such inquiries or requests should be directed to:

1065 [ganzer@battelle.org](mailto:ganzer@battelle.org).

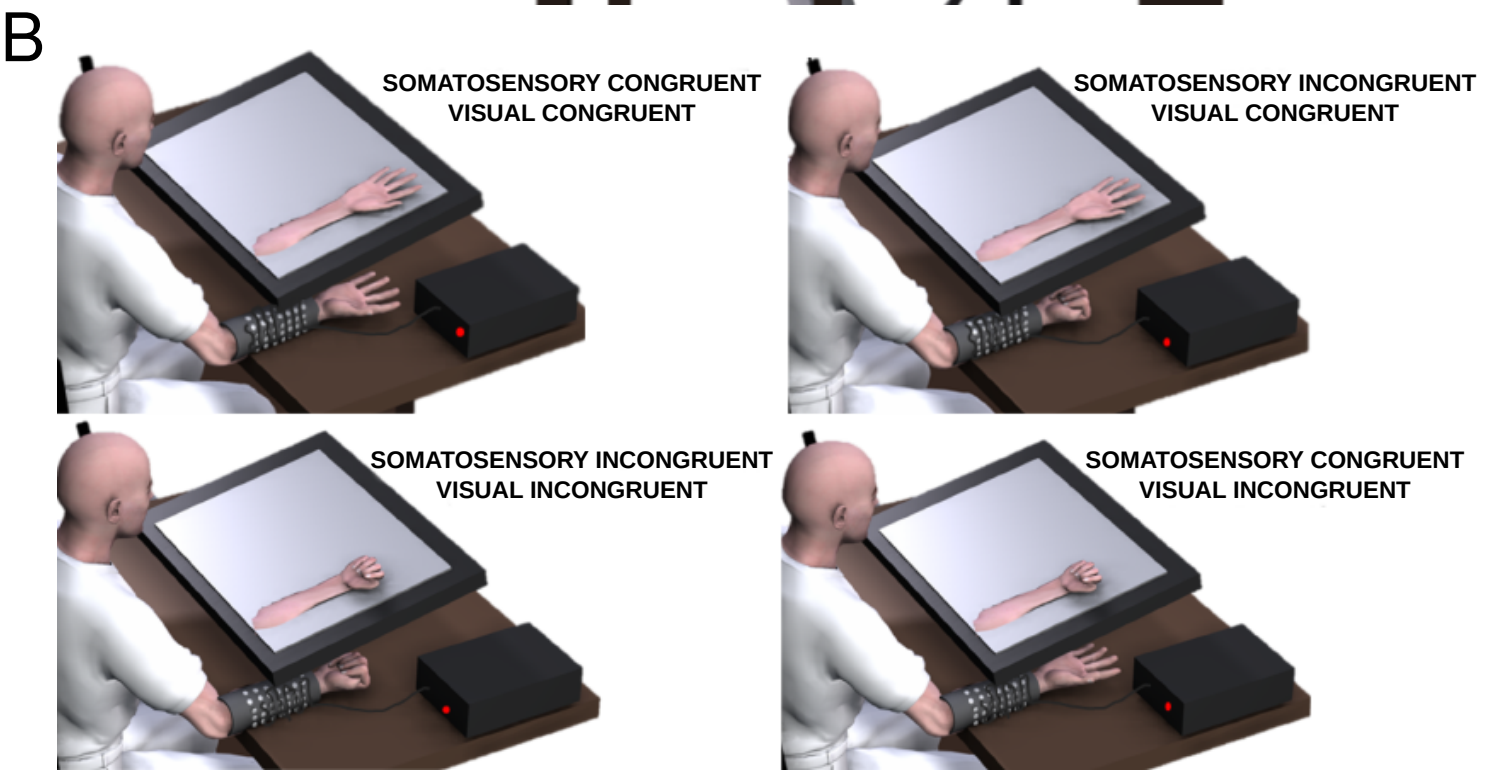
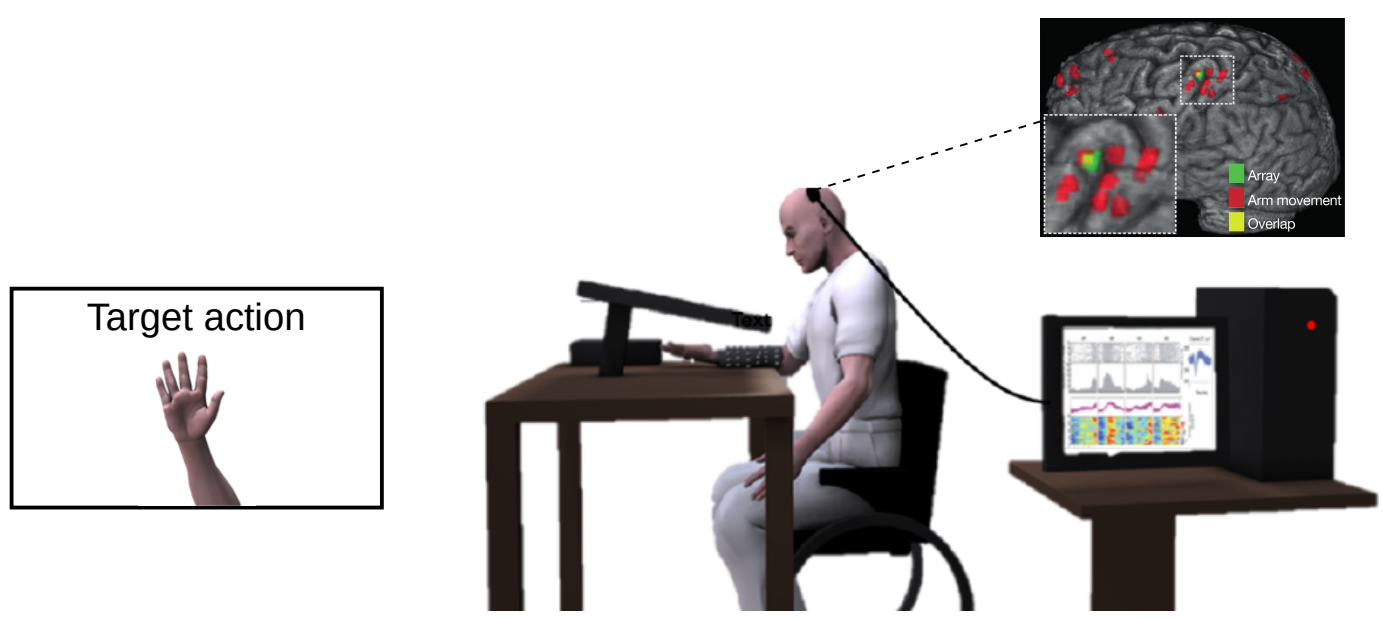
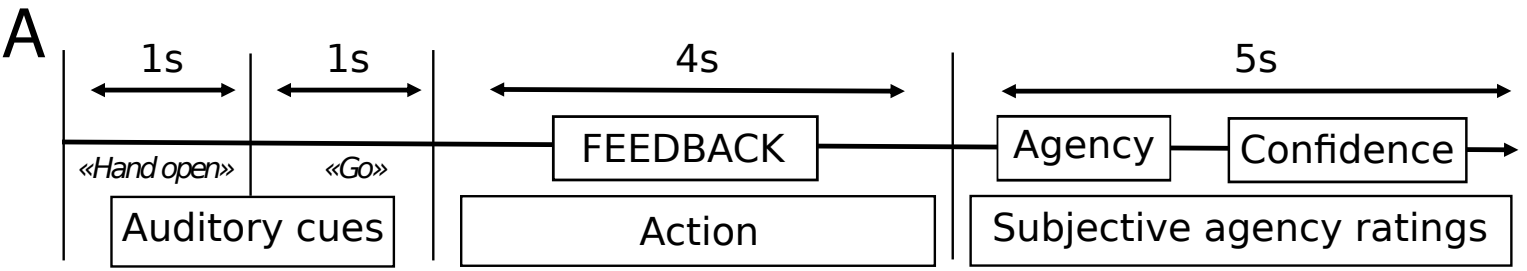
1066

### 1067 **Code availability statement**

1068

1069 Custom code for neural data analysis and BMI control can be obtained following a  
1070 written agreement between Battelle Memorial Institute and the requester's affiliated  
1071 institution. Such inquiries or requests should be directed to: [ganzer@battelle.org](mailto:ganzer@battelle.org).  
1072 Inquiries or requests concerning custom analysis code used for this study should be  
1073 directed to AS.

1074

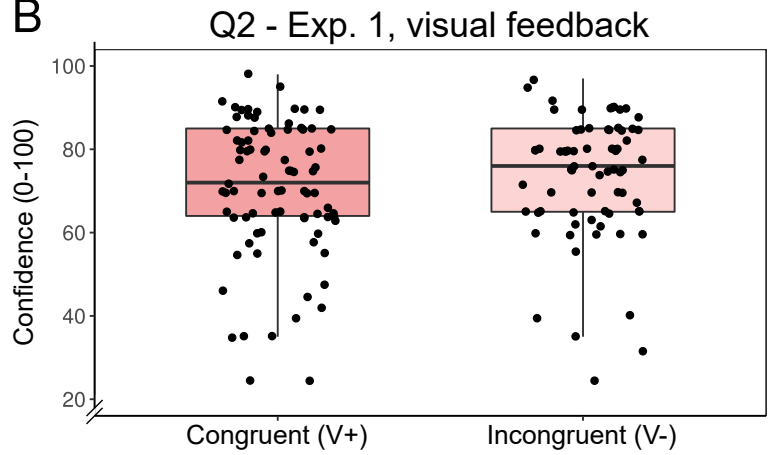
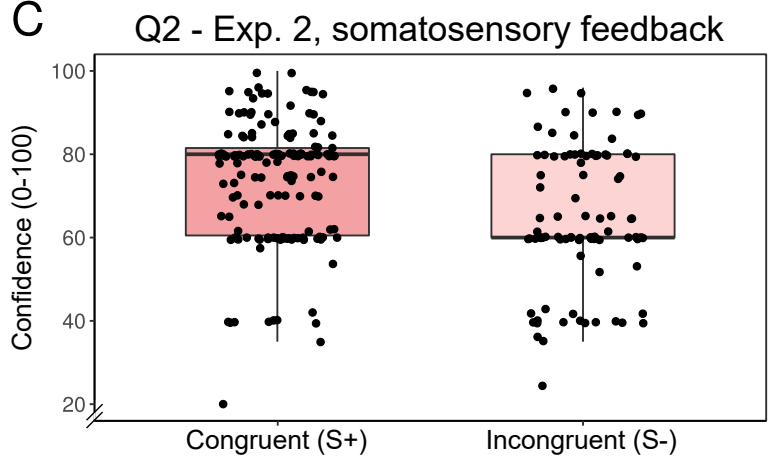
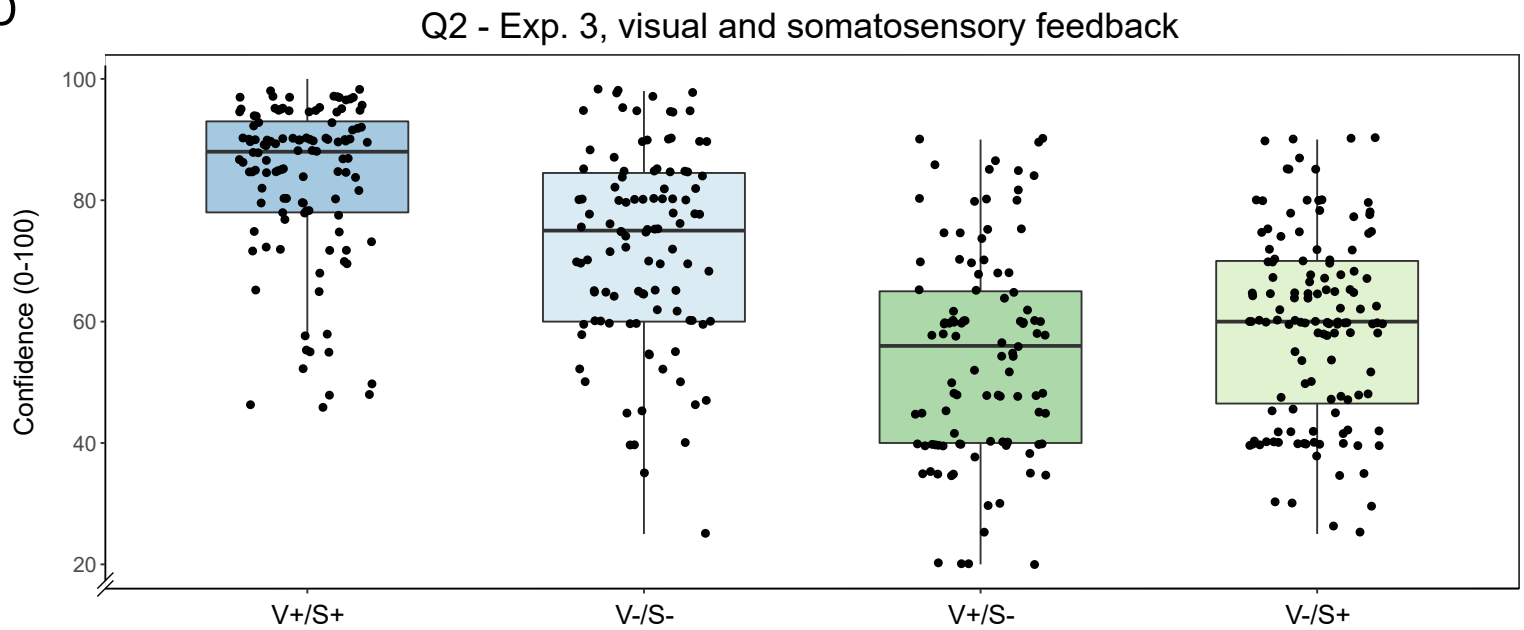


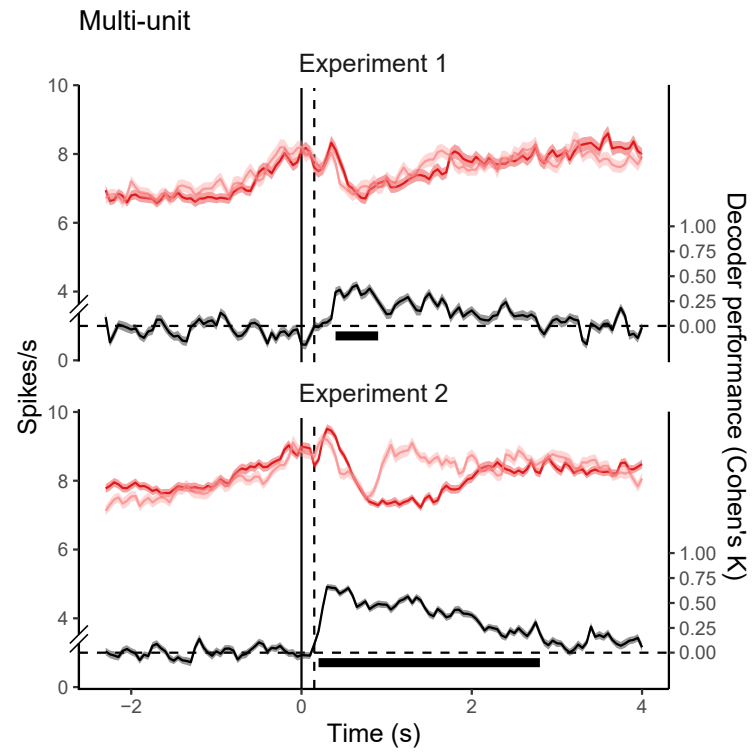
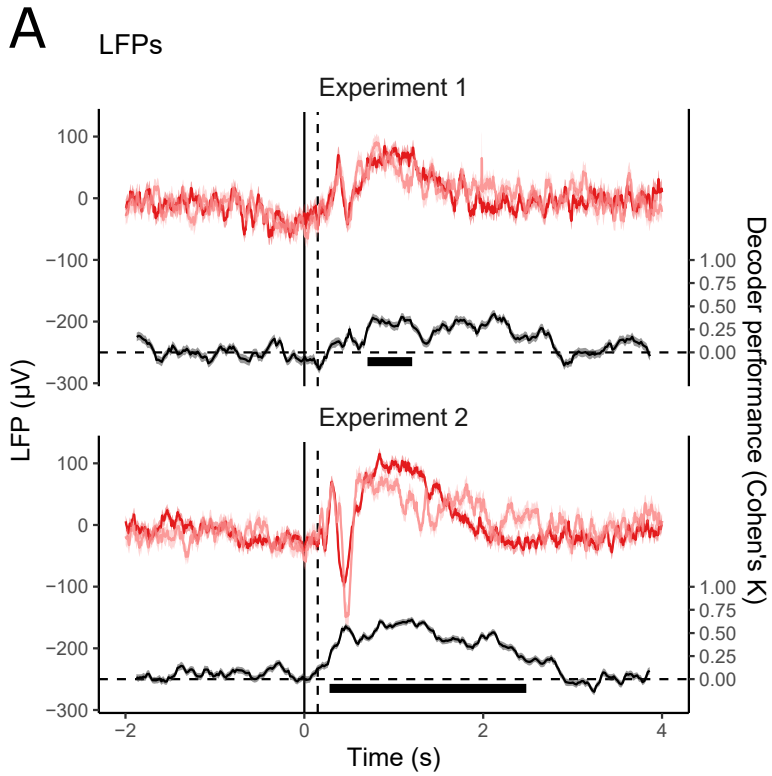
**A**

Q1, % of "Yes" answers

Visual feedback

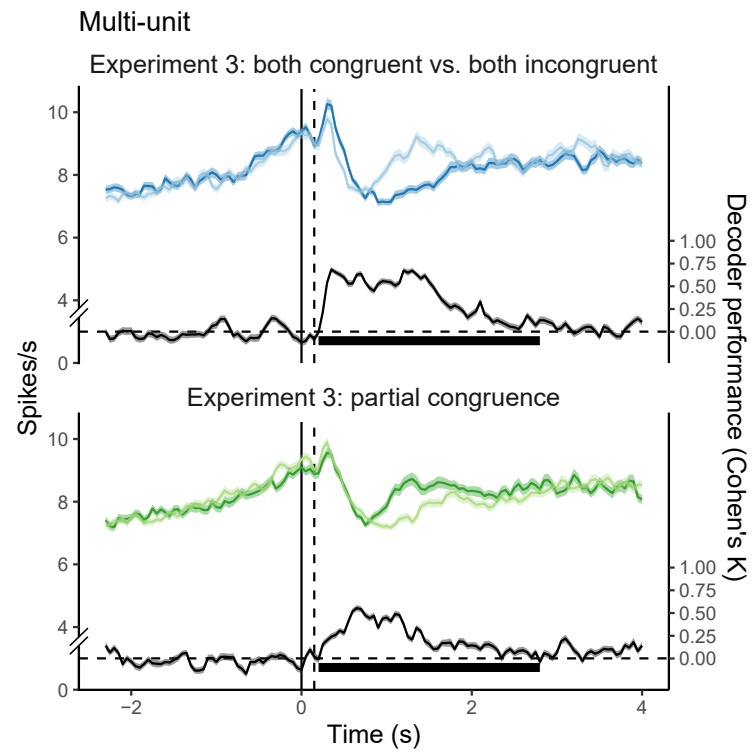
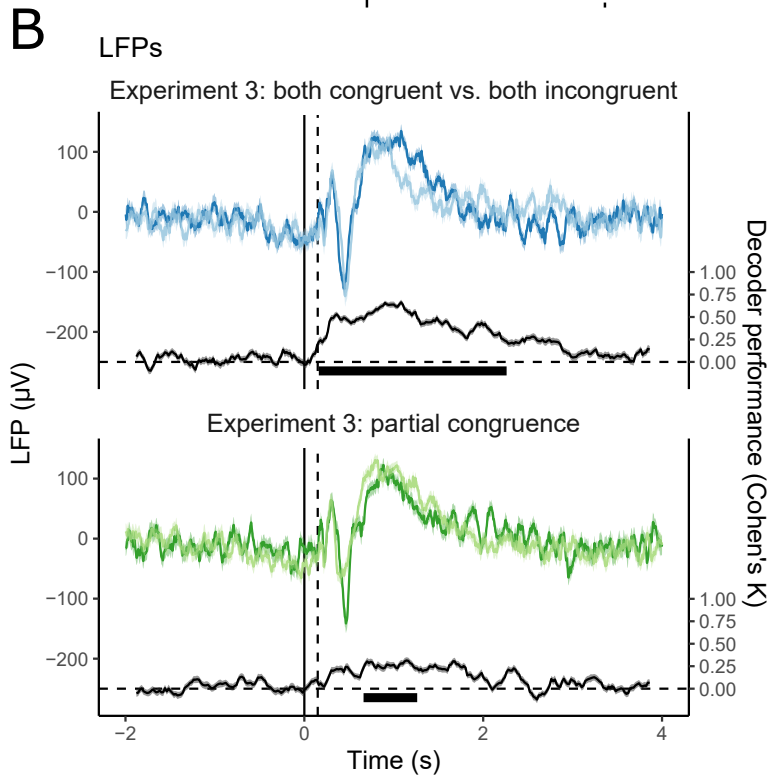
		Congruent (+)	None	Incongruent (-)
Somatosensory feedback	Congruent (+)	Exp. 3 100 %	Exp. 2 97.4 %	Exp. 3 68.5 %
	None	Exp. 1 94 %		Exp. 1 5.6 %
	Incongruent (-)	Exp. 3 52.5 %	Exp. 2 9 %	Exp. 3 7.8 %

**B****C****D**



Feedback

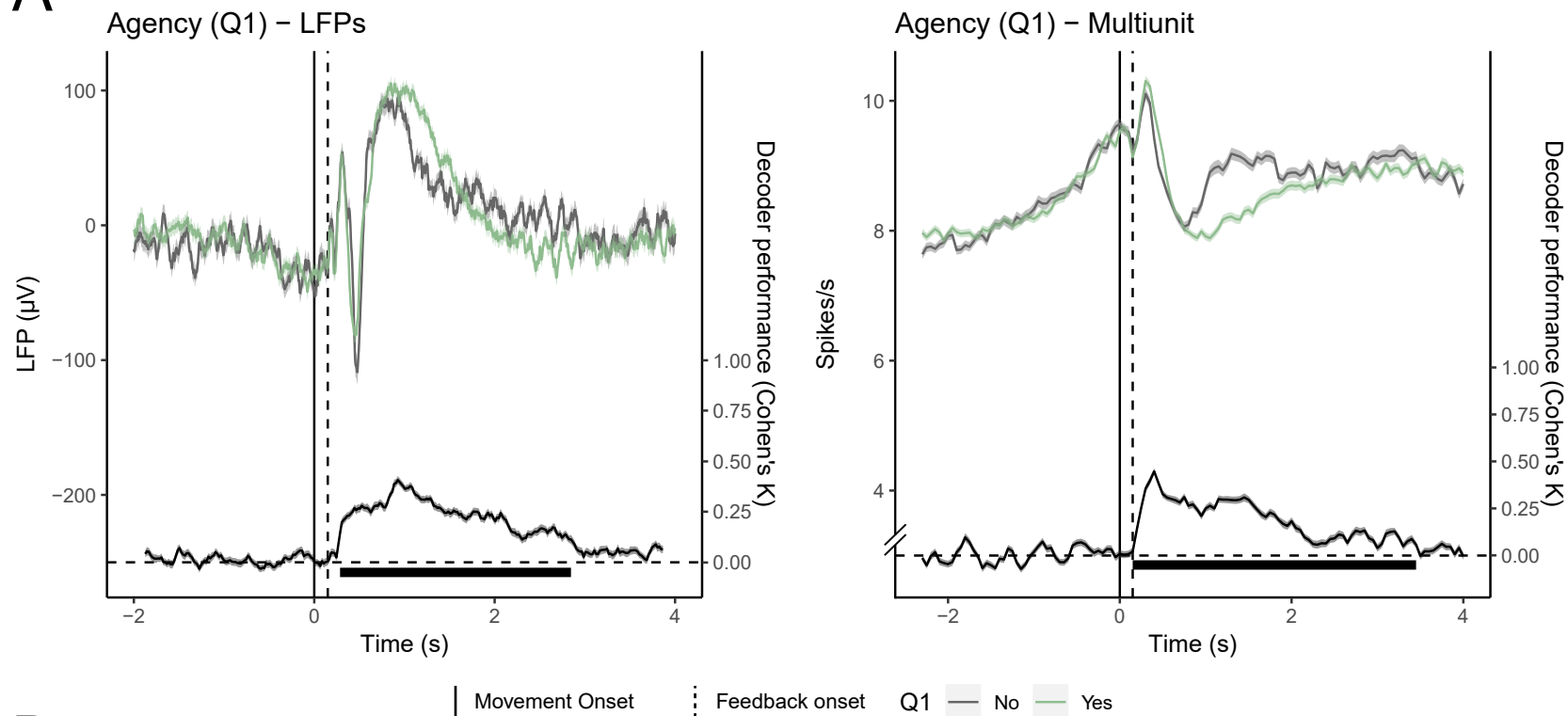
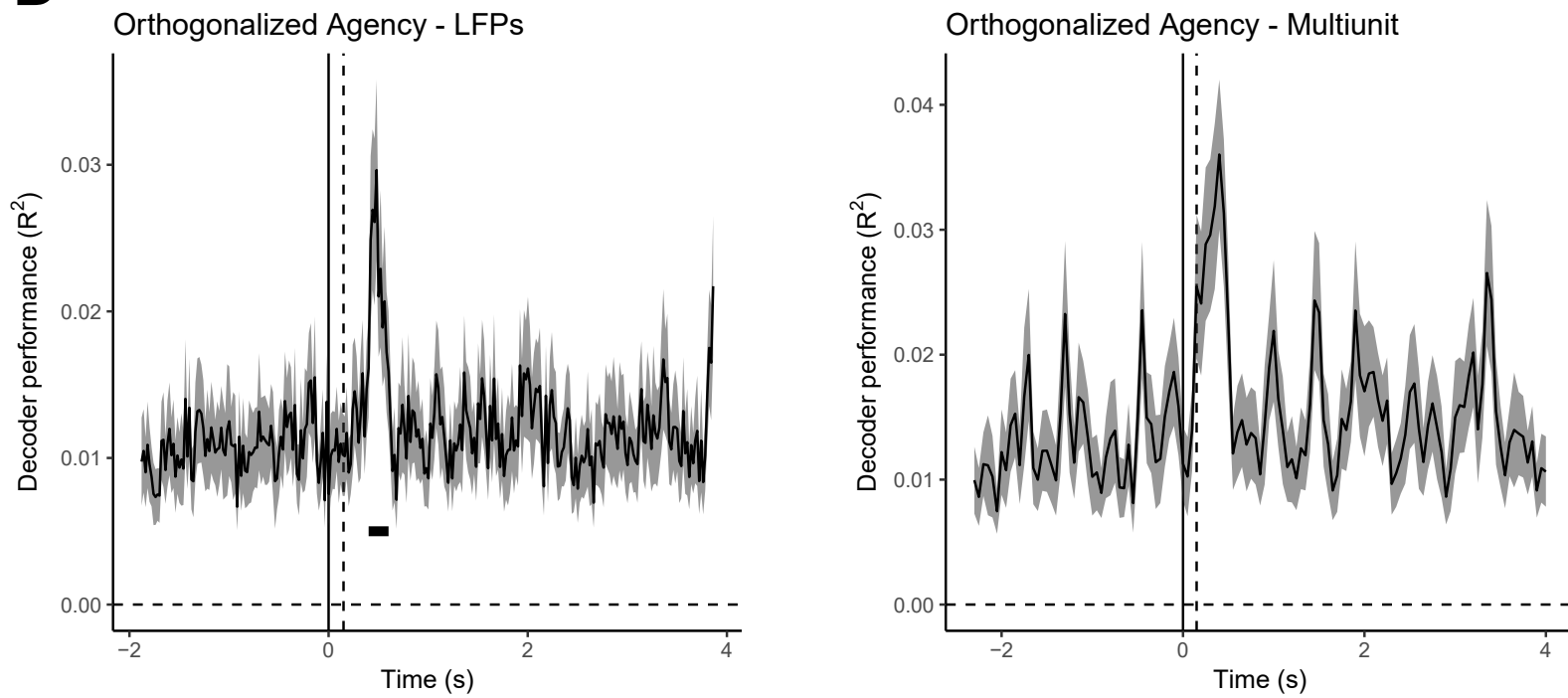
— Congruent (V+ or S+) — Incongruent (V- or S-)

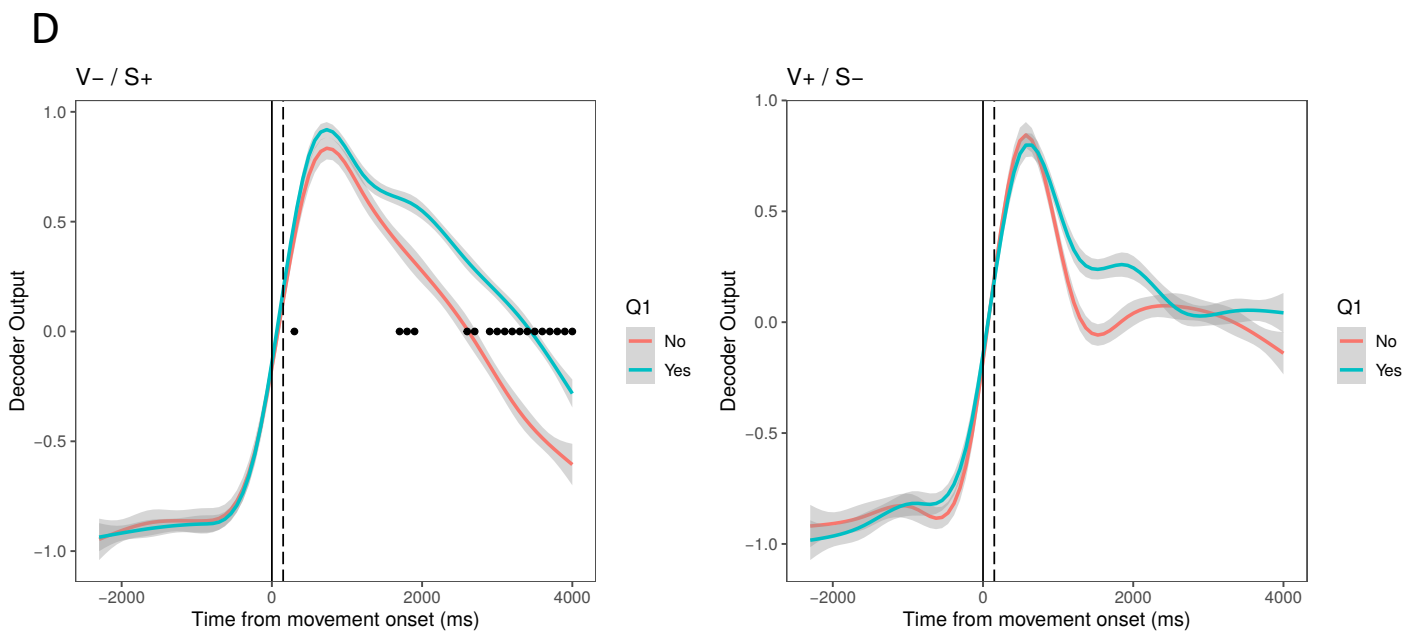
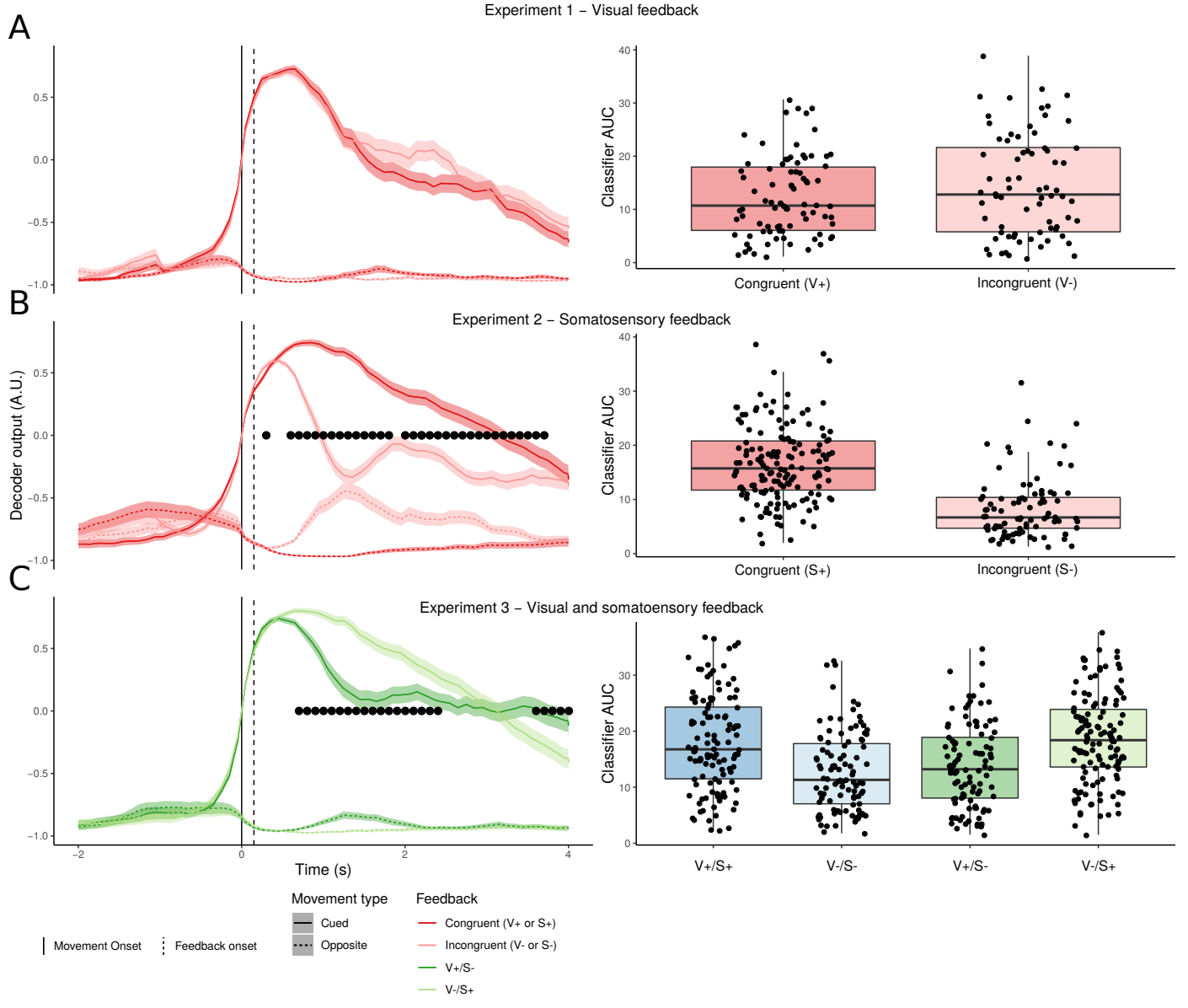


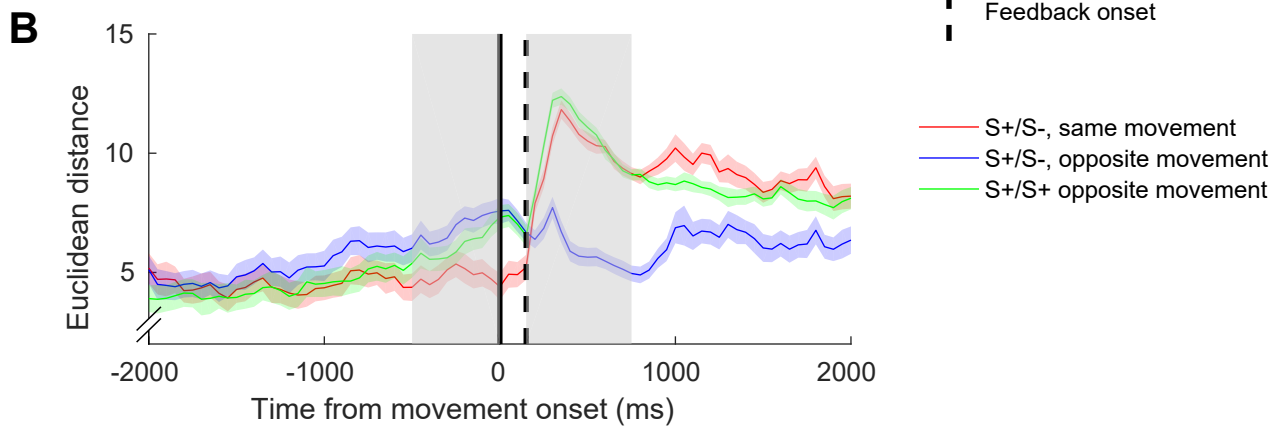
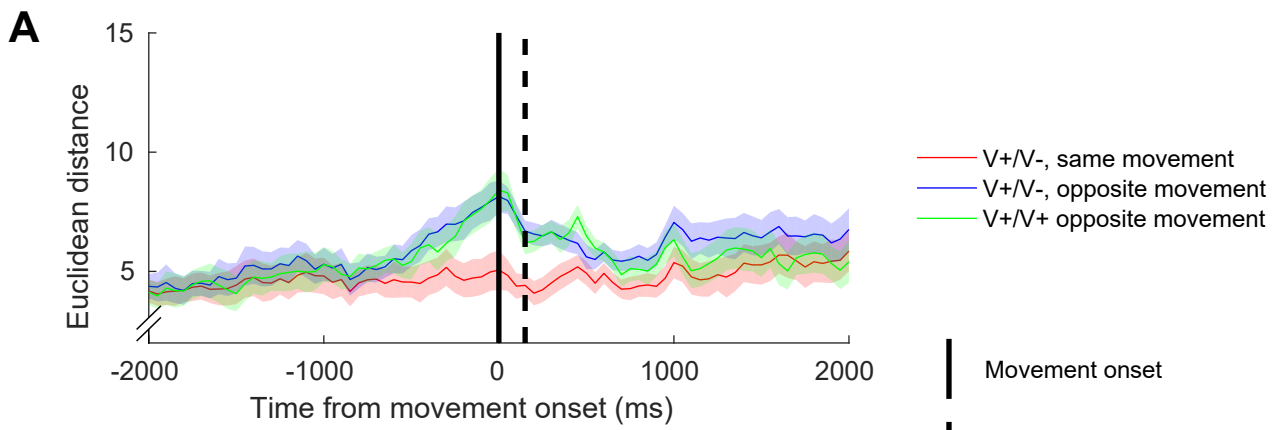
Feedback

— V+/S+ — V-/S-  
— V+/S- — V-/S+

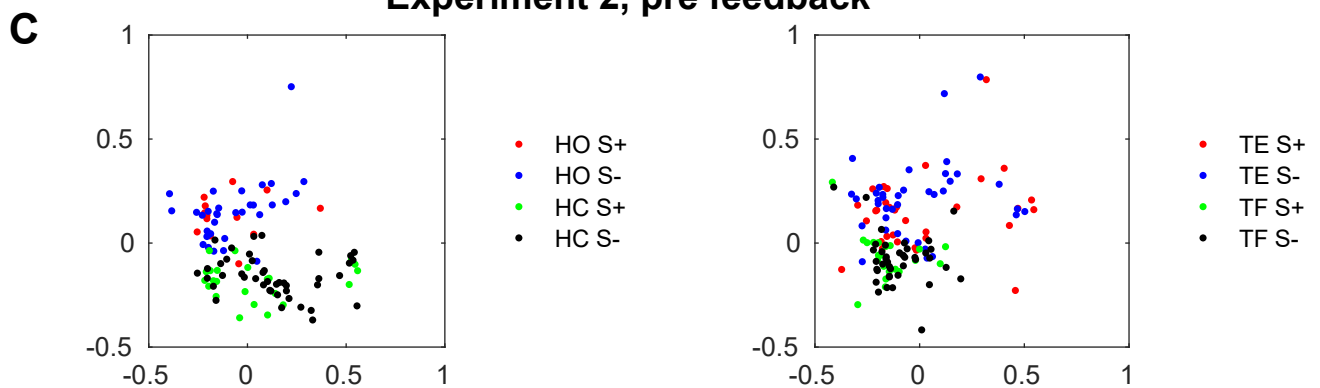


**A****B**





**Experiment 2, pre feedback**



**Experiment 2, post feedback**

